



CHORUS

This is the accepted manuscript made available via CHORUS. The article has been published as:

Quasiparticle equation of state for anisotropic hydrodynamics

Mubarak Alqahtani, Mohammad Nopoush, and Michael Strickland

Phys. Rev. C **92**, 054910 — Published 23 November 2015

DOI: [10.1103/PhysRevC.92.054910](https://doi.org/10.1103/PhysRevC.92.054910)

Quasiparticle equation of state for anisotropic hydrodynamics

Mubarak Alqahtani, Mohammad Nopoush, and Michael Strickland

Department of Physics, Kent State University, Kent, OH 44242 United States

(Dated: September 14, 2015)

Abstract

We present a new method for imposing a realistic equation of state in anisotropic hydrodynamics. The method relies on the introduction of a single finite-temperature quasiparticle mass which is fit to lattice data. By taking moments of the Boltzmann equation, we obtain a set of coupled partial differential equations which can be used to describe the 3+1d spacetime evolution of an anisotropic relativistic system. We then specialize to the case of a 0+1d system undergoing boost-invariant Bjorken expansion and subject to the relaxation-time approximation collisional kernel. Using this setup, we compare results obtained using the new quasiparticle equation of state method with those obtained using the standard method for imposing the equation of state in anisotropic hydrodynamics. We demonstrate that the temperature evolution obtained using the two methods is nearly identical and that there are only small differences in the pressure anisotropy. However, we find that there are significant differences in the evolution of the bulk pressure correction.

PACS numbers: 12.38.Mh, 24.10.Nz, 25.75.-q, 51.10.+y, 52.27.Ny

Keywords: Quark-gluon plasma, Relativistic heavy-ion collisions, Anisotropic hydrodynamics, Equation of state, Quasiparticle model, Boltzmann equation

20 I. INTRODUCTION

21 Ultrarelativistic heavy-ion collision experiments using the Relativistic Heavy Ion Collider
22 (RHIC) at Brookhaven National Laboratory and the Large Hadron Collider (LHC) at CERN
23 allow researchers to study the behavior of matter subject to extreme conditions. In these
24 experiments, high-energy collisions of nuclei are used to heat a tiny volume of matter up
25 to temperatures that exceed the critical temperature ($T_c \sim 160$ MeV) necessary to create a
26 super-hot deconfined and chirally-symmetric phase, called the quark-gluon plasma (QGP).
27 The study of this strongly interacting phase near and above the critical temperature is of
28 fundamental interest. One can gain some insight into the physics of the QGP using per-
29 turbation theory since the asymptotic freedom of quantum chromodynamics (QCD) ensures
30 that, for the high temperatures, $T \gg \Lambda_{\text{QCD}}$, the QGP can be thought of as a weakly-
31 coupled many-body system. In this regime, perturbative methods, such as hard thermal
32 loop (HTL) resummation, can be used [1–6].¹ In the HTL framework, the quarks and glu-
33 ons can be thought of as quasiparticles having temperature-dependent (thermal) masses
34 with $m_{q,\bar{q},g} \sim gT$, where g is the strong coupling.

35 Such a picture provides motivation to try to model the QGP as a gas of massive quasipar-
36 ticles for the purposes of obtaining self-consistent hydrodynamic equations. However, per-
37 turbation theory needs to be supplemented since, for temperatures $T \lesssim 2T_c$, first-principles
38 perturbative calculations based on deconfined quarks and gluons break down. In order
39 to proceed, one can use non-perturbative lattice calculations of QCD thermodynamics to
40 determine information about the necessary quasiparticle mass(es). In practice, one can
41 perform this procedure at all temperatures and determine a non-perturbative temperature-
42 dependent quasiparticle mass, $m(T)$. Once $m(T)$ is determined, one can use this to enforce
43 the target equation of state (EoS) in an effective kinetic field theory framework. One compli-
44 cation is that, in order to guarantee thermodynamic consistency in equilibrium and related
45 out-of-equilibrium constraints, it is necessary to introduce a background (vacuum energy)
46 contribution to the energy-momentum tensor [9–11]. The resulting EoS, together with a self-
47 consistent non-equilibrium energy-momentum tensor and modified Boltzmann equation, can
48 be used to derive relativistic hydrodynamic equations for such a quasiparticle gas.

49 Relativistic hydrodynamics itself is an effective theory that can be used to describe the

¹HTL-resummed calculations of the thermodynamic potential at finite temperature and quark chemical potential(s) describe the lattice data well for $T \gtrsim 300$ MeV with no free parameters [6–8].

50 spacetime evolution of the QGP. In the kinetic theory approach to relativistic hydrody-
51 namics, one obtains the dynamical equations for the bulk variables by taking moments of
52 the Boltzmann equation. Ideal hydrodynamics [12–14] and later on viscous hydrodynamics
53 [15–46] have been used to study the QGP created in heavy-ion collisions and have proven
54 to be quite successful. Recently, anisotropic hydrodynamics [47–68] has been developed
55 in order to extend the range of applicability of relativistic hydrodynamics to situations in
56 which the QGP possess a high degree of momentum-space anisotropy (for a recent review,
57 see Ref. [69]).

58 In most cases, however, the manner in which the EoS is imposed in hydrodynamics is
59 somewhat uncontrolled. In many cases, one derives the hydrodynamic equations for a con-
60 formal system and then imposes an EoS to relate the components of the energy-momentum
61 tensor. We refer to this as the “standard EoS” method. However, since QCD is a non-
62 conformal theory with a running coupling constant that depends strongly on the temperature
63 near T_c , it is more self-consistent to take into account the breaking of conformal invariance
64 from the beginning, which results in additional terms in the evolution equations and new
65 transport coefficients. Some progress in this direction has been made in the last year, both
66 in the context of second-order viscous hydrodynamics [44] and anisotropic hydrodynamics
67 [62], however, in both of these previous works, the underlying microscopic picture was that
68 of a gas of particles with temperature-independent masses. One would like to incorporate
69 the temperature-dependence of the particle masses into the dynamical equations such that
70 the equations themselves are consistent with the breaking of conformal invariance and the
71 quasiparticle picture at high temperatures. In this paper, we present a method for doing
72 this in the context of anisotropic hydrodynamics. Our method is to incorporate the effects
73 of a temperature-dependent quasiparticle mass into the Boltzmann equation by taking into
74 account extra terms which come from the spacetime gradients of the thermal mass. We
75 show that adding the necessary additional term to the Boltzmann equation and enforcing
76 energy-momentum conservation require one to introduce a non-equilibrium background field
77 $Bg^{\mu\nu}$ to the energy-momentum tensor as was found by previous authors [10, 11], e.g.

$$T^{\mu\nu} = T_{\text{kinetic}}^{\mu\nu} + Bg^{\mu\nu} . \quad (1)$$

78 This extra background contribution can be shown to become precisely the additional term

79 necessary to enforce thermodynamic consistency in the equilibrium limit, however, in prac-
80 tice, we allow it to be a non-equilibrium quantity.

81 The new method above will be referred to herein as the “quasiparticle EoS”. We com-
82 pare results obtained using this method to results obtained using the canonical method for
83 imposing a realistic equation of state. For this purpose, we reduce the dynamical equations
84 in both cases to those appropriate for 0+1d boost-invariant and transversally-homogeneous
85 expansion subject to a relaxation-time approximation collisional kernel. With this setup,
86 comparisons of the evolution of the effective temperature, pressure anisotropy, and bulk
87 correction to the pressure for different values of the shear viscosity to entropy density ratio
88 are presented for both isotropic and anisotropic initial conditions. We demonstrate that
89 the temperature evolution obtained using the two EoS methods is nearly identical and that
90 there are only small differences in the pressure anisotropy. However, we find that there are
91 significant differences in the evolution of the bulk pressure correction, which could poten-
92 tially be important for determining the correct form of the particle distribution function on
93 the freezeout hypersurface in phenomenological applications.

94 The structure of the paper is as follows. In Sec. II, we present the notation and conventions
95 we use in the paper. In Sec. III, we review the necessary setup including the anisotropic dis-
96 tribution function, basis vectors necessary in different cases, and the lattice-based equation
97 of state we will use. In Sec. IV, the Boltzmann equation and its generalization to quasiparti-
98 cles with temperature-dependent masses is discussed. In Sec. V, we take different moments
99 of distribution function in order to derive expressions for the particle current, energy den-
100 sity, and components of the pressure. In Sec. VI, the 3+1d dynamical equations for mas-
101 sive anisotropic hydrodynamics are derived and then simplified assuming boost-invariance
102 together with either cylindrical-symmetry or transversally-homogeneity. In Sec. VII, we
103 obtain the 0+1d dynamical equations for the quasiparticle EoS and standard EoS cases.
104 In Sec. VIII, our numerical results obtained using both methods for a boost-invariant and
105 transversally-homogeneous system are presented. Sec. IX contains our conclusions and an
106 outlook for the future. All necessary identities and function definitions are collected in
107 Apps. A-B.

108 **II. CONVENTIONS AND NOTATION**

109 A parentheses in the indices indicates a symmetrized form, e.g. $A^{(\mu\nu)} \equiv (A^{\mu\nu} + A^{\nu\mu})/2$.
 110 The metric is taken to be “mostly minus” such that in Minkowski space with $x^\mu \equiv (t, x, y, z)$
 111 the line element is $ds^2 = g_{\mu\nu} dx^\mu dx^\nu = dt^2 - dx^2 - dy^2 - dz^2$. We also make use of the transverse
 112 projector, $\Delta^{\mu\nu} \equiv g^{\mu\nu} - u^\mu u^\nu$. When studying relativistic heavy-ion collisions, it is convenient
 113 to transform to variables defined by $\tau = \sqrt{t^2 - z^2}$, which is the longitudinal proper time, and
 114 $\varsigma = \tanh^{-1}(z/t)$, which is the longitudinal spacetime rapidity. If the system is additionally
 115 cylindrically symmetric with respect to the beam-line, it is convenient to transform to polar
 116 coordinates in the transverse plane with $r = \sqrt{x^2 + y^2}$ and $\phi = \tan^{-1}(y/x)$. In this case, the
 117 new set of coordinates $x^\mu = (\tau, r, \phi, \varsigma)$ defines polar Milne coordinates. Finally, the invariant
 118 phase space integration measure is defined as

$$dP \equiv N_{\text{dof}} \frac{d^3p}{(2\pi)^3} \frac{1}{E} = \tilde{N} \frac{d^3p}{E}, \quad (2)$$

119 where N_{dof} is the number of degrees of freedom and $\tilde{N} \equiv N_{\text{dof}}/(2\pi)^3$.

120 **III. SETUP**

121 In this paper, we derive non-conformal anisotropic hydrodynamics equations for a sys-
 122 tem of quasiparticles with a temperature-dependent mass. To accomplish this goal, an
 123 effective Boltzmann equation for thermal quasiparticles is obtained. We then take moments
 124 of the resulting kinetic equation to obtain the leading-order 3+1d anisotropic hydrodynam-
 125 ics equations. Using a general set of basis vectors, the equations are expanded explicitly
 126 and then various simplifying assumptions (e.g. boost-invariance, etc.) are imposed to re-
 127 duce the equations from their general 3+1d to a 0+1d form appropriate for describing a
 128 boost-invariant and transversally-homogenous QGP. The obtained 0+1d equations are then
 129 solved numerically for our tests, however, the method used to obtain the 3+1d leading-order
 130 anisotropic hydrodynamics equations can be used without lack of generality.

131 **A. Basis Vectors**

132 A general tensor basis can be constructed by introducing four four-vectors which in the
 133 local rest frame (LRF) are

$$\begin{aligned}
 u_{\text{LRF}}^\mu &\equiv (1, 0, 0, 0), \\
 X_{\text{LRF}}^\mu &\equiv (0, 1, 0, 0), \\
 Y_{\text{LRF}}^\mu &\equiv (0, 0, 1, 0), \\
 Z_{\text{LRF}}^\mu &\equiv (0, 0, 0, 1).
 \end{aligned}
 \tag{3}$$

134 One can define the general basis vectors in the lab frame (LF) by performing the Lorentz
 135 transformation necessary to go from LRF to the LF. The transformation required can be
 136 constructed using a longitudinal boost ϑ along the beam axis, followed by a rotation φ
 137 around the beam axis, and finally a transverse boost by θ_\perp along the x -axis [52, 53]. This
 138 parametrization gives

$$\begin{aligned}
 u^\mu &\equiv (\cosh \theta_\perp \cosh \vartheta, \sinh \theta_\perp \cos \varphi, \sinh \theta_\perp \sin \varphi, \cosh \theta_\perp \sinh \vartheta), \\
 X^\mu &\equiv (\sinh \theta_\perp \cosh \vartheta, \cosh \theta_\perp \cos \varphi, \cosh \theta_\perp \sin \varphi, \sinh \theta_\perp \sinh \vartheta), \\
 Y^\mu &\equiv (0, -\sin \varphi, \cos \varphi, 0), \\
 Z^\mu &\equiv (\sinh \vartheta, 0, 0, \cosh \vartheta),
 \end{aligned}
 \tag{4}$$

139 where the three fields ϑ , φ , and θ_\perp are functions of Cartesian Milne coordinates (τ, x, y, ς) .
 140 Introducing another parametrization by using the temporal and transverse components of
 141 flow velocity

$$u_0 = \cosh \theta_\perp, \tag{5}$$

$$u_x = u_\perp \cos \varphi, \tag{6}$$

$$u_y = u_\perp \sin \varphi, \tag{7}$$

142 where $u_{\perp} \equiv \sqrt{u_x^2 + u_y^2} = \sqrt{u_0^2 - 1} = \sinh \theta_{\perp}$, one has

$$\begin{aligned}
u^{\mu} &\equiv (u_0 \cosh \vartheta, u_x, u_y, u_0 \sinh \vartheta), \\
X^{\mu} &\equiv \left(u_{\perp} \cosh \vartheta, \frac{u_0 u_x}{u_{\perp}}, \frac{u_0 u_y}{u_{\perp}}, u_{\perp} \sinh \vartheta \right), \\
Y^{\mu} &\equiv \left(0, -\frac{u_y}{u_{\perp}}, \frac{u_x}{u_{\perp}}, 0 \right), \\
Z^{\mu} &\equiv (\sinh \vartheta, 0, 0, \cosh \vartheta).
\end{aligned} \tag{8}$$

143 For a boost-invariant and cylindrically-symmetric system, one can simplify the basis vectors
144 by identifying $\vartheta = \varsigma$ and $\varphi = \phi$ where ς and ϕ are the spacetime rapidity and the azimuthal
145 angle, respectively. In this case, the basis vectors (4) simplify to

$$\begin{aligned}
u^{\mu} &= (\cosh \theta_{\perp} \cosh \varsigma, \sinh \theta_{\perp} \cos \phi, \sinh \theta_{\perp} \sin \phi, \cosh \theta_{\perp} \sinh \varsigma), \\
X^{\mu} &= (\sinh \theta_{\perp} \cosh \varsigma, \cosh \theta_{\perp} \cos \phi, \cosh \theta_{\perp} \sin \phi, \sinh \theta_{\perp} \sinh \varsigma), \\
Y^{\mu} &= (0, -\sin \phi, \cos \phi, 0), \\
Z^{\mu} &= (\sinh \varsigma, 0, 0, \cosh \varsigma).
\end{aligned} \tag{9}$$

146 In the case of a transversally-symmetric system, the transverse flow u_{\perp} is absent, i.e. $\theta_{\perp} = 0$,
147 and, as a consequence, one has

$$\begin{aligned}
u^{\mu} &= (\cosh \varsigma, 0, 0, \sinh \varsigma), \\
X^{\mu} &= (0, \cos \phi, \sin \phi, 0), \\
Y^{\mu} &= (0, -\sin \phi, \cos \phi, 0), \\
Z^{\mu} &= (\sinh \varsigma, 0, 0, \cosh \varsigma).
\end{aligned} \tag{10}$$

148 Note that in the last case, X^{μ} and Y^{μ} are simply unit vectors pointing along the radial and
149 azimuthal directions, respectively.

150 **B. Ellipsoidal form including bulk pressure degree of freedom**

151 In the non-conformal case, anisotropic hydrodynamics is defined through the introduction
 152 of an anisotropy tensor of the form [53, 62]

$$\Xi^{\mu\nu} = u^\mu u^\nu + \xi^{\mu\nu} - \Delta^{\mu\nu} \Phi, \quad (11)$$

153 where u^μ is four-velocity, $\xi^{\mu\nu}$ is a symmetric and traceless tensor, and Φ is associated with
 154 the bulk degree of freedom. The quantities u^μ , $\xi^{\mu\nu}$, and Φ are understood to be functions
 155 of spacetime and obey $u^\mu u_\mu = 1$, $\xi^\mu{}_\mu = 0$, $\Delta^\mu{}_\mu = 3$, and $u_\mu \xi^{\mu\nu} = 0$; therefore, one has
 156 $\Xi^\mu{}_\mu = 1 - 3\Phi$. At leading order in the anisotropic hydrodynamics expansion one assumes
 157 that the one-particle distribution function is of the form

$$f(x, p) = f_{\text{iso}} \left(\frac{1}{\lambda} \sqrt{p_\mu \Xi^{\mu\nu} p_\nu} \right), \quad (12)$$

158 where λ has dimensions of energy and can be identified with the temperature only in the
 159 isotropic equilibrium limit ($\xi^{\mu\nu} = 0$ and $\Phi = 0$).² We note that, in practice, f_{iso} need
 160 not be a thermal equilibrium distribution. However, unless one expects there to be a non-
 161 thermal distribution at late times, it is appropriate to take f_{iso} to be a thermal equilibrium
 162 distribution function of the form $f_{\text{iso}}(x) = f_{\text{eq}}(x) = (e^x + a)^{-1}$, where $a = \pm 1$ gives Fermi-
 163 Dirac or Bose-Einstein statistics, respectively, and $a = 0$ gives Boltzmann statistics. From
 164 here on, we assume that the distribution is of Boltzmann form, i.e. $a = 0$.

165 **C. Dynamical Variables**

166 Since the most important viscous corrections are to the diagonal components of the
 167 energy-momentum tensor, to good approximation one can assume that $\xi^{\mu\nu} = \text{diag}(0, \boldsymbol{\xi})$ with
 168 $\boldsymbol{\xi} \equiv (\xi_x, \xi_y, \xi_z)$ and $\xi_i^i = 0$. In this case, expanding the argument of the square root appearing
 169 on the right-hand side of Eq. (12) in the LRF gives

$$f(x, p) = f_{\text{eq}} \left(\frac{1}{\lambda} \sqrt{\sum_i \frac{p_i^2}{\alpha_i^2} + m^2} \right), \quad (13)$$

²Herein we assume that the chemical potential is zero.

170 where $i \in \{x, y, z\}$ and the scale parameters α_i are

$$\alpha_i \equiv (1 + \xi_i + \Phi)^{-1/2}. \quad (14)$$

171 Note that, for brevity, one can collect the three anisotropy parameters into vector $\boldsymbol{\alpha} \equiv$
 172 $(\alpha_x, \alpha_y, \alpha_z)$. In the isotropic equilibrium limit, where $\xi_i = \Phi = 0$ and $\alpha_i = 1$, one has
 173 $p_\mu \Xi^{\mu\nu} p_\nu = (p \cdot u)^2 = E^2$ and $\lambda \rightarrow T$ and, therefore,

$$f(x, p) = f_{\text{eq}}\left(\frac{E}{T(x)}\right). \quad (15)$$

174 Out of the four anisotropy and bulk parameters there are only three independent ones. In
 175 practice, we use three variables α_i as the dynamical anisotropy parameters since, by using
 176 Eq. (14) and the tracelessness of $\xi^{\mu\nu}$, one can write Φ in terms of the anisotropy parameters,
 177 $\Phi = \frac{1}{3} \sum_i \alpha_i^{-2} - 1$. In the transversally-homogeneous case, one has $\alpha_x = \alpha_y$ and, as a result,
 178 there are two independent anisotropy parameters. Note that, for conformal systems, one
 179 has $\Phi = 0$ and in this case there are then only two independent anisotropy parameters in
 180 3+1d.

181 D. Equation of state

182 Herein we consider a system at finite temperature and zero chemical potential. At asymp-
 183 totically high temperatures, the pressure of a gas of quarks and gluons approaches the Stefan-
 184 Boltzmann (SB) limit, $\mathcal{P}_{\text{SB}} = \mathcal{E}_{\text{SB}}/3 = N_{\text{dof}} T^4 / \pi^2 = \pi^2 T^4 (N_c^2 - 1 + \frac{7}{4} N_c N_f) / 45$. We will
 185 take $N_c = N_f = 3$ in what follows. At the temperatures probed in heavy-ion collisions there
 186 are important corrections to the SB limit and at low temperatures the relevant degrees of
 187 freedom change from quarks and gluons to hadrons. The standard way to determine the
 188 QGP EoS is to use non-perturbative lattice calculations. For this purpose, we use an an-
 189 alytic parameterization of lattice data for the QCD interaction measure (trace anomaly),
 190 $I_{\text{eq}} = \mathcal{E}_{\text{eq}} - 3\mathcal{P}_{\text{eq}}$, taken from the Wuppertal-Budapest collaboration [70]

$$\frac{I_{\text{eq}}(T)}{T^4} = \left[\frac{h_0}{1 + h_3 t^2} + \frac{f_0 [\tanh(f_1 t + f_2) + 1]}{1 + g_1 t + g_2 t^2} \right] \exp\left(-\frac{h_1}{t} - \frac{h_2}{t^2}\right), \quad (16)$$

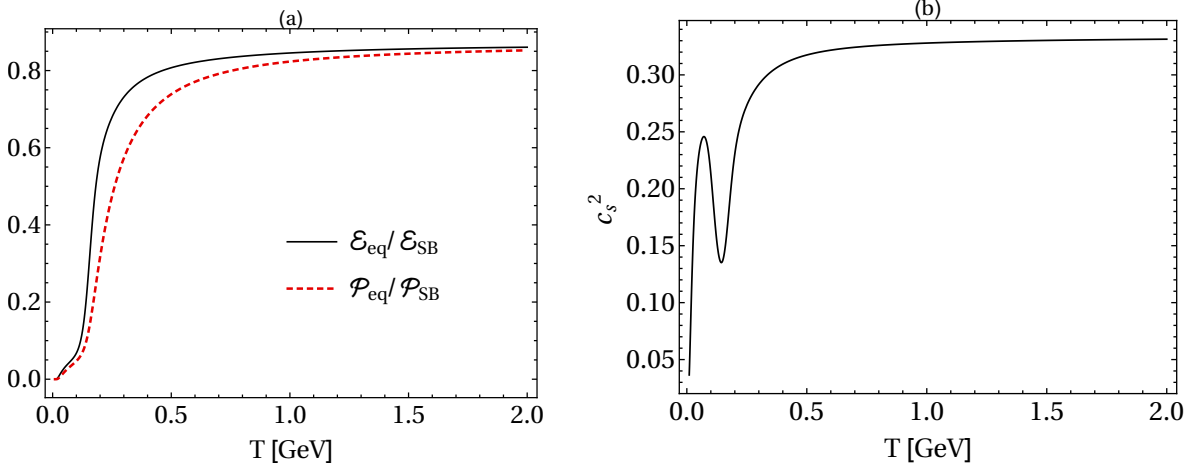


FIG. 1. Panel (a) shows the energy density and pressure scaled by their respective Stefan-Boltzmann limits as a function of temperature. Panel (b) shows the speed of sound squared as a function of temperature.

191 with $t \equiv T/(0.2 \text{ GeV})$. For $N_f = 2 + 1$ (2 light quarks and one heavy quark) the parameters
 192 are $h_0 = 0.1396$, $h_1 = -0.1800$, $h_2 = 0.0350$, $f_0 = 2.76$, $f_1 = 6.79$, $f_2 = -5.29$, $g_1 = -0.47$,
 193 $g_2 = 1.04$, and $h_3 = 0.01$.

194 The pressure can be obtained from an integral of the interaction measure

$$\frac{\mathcal{P}_{\text{eq}}(T)}{T^4} = \int_0^T \frac{dT}{T} \frac{I_{\text{eq}}(T)}{T^4}, \quad (17)$$

195 where we have assumed $\mathcal{P}_{\text{eq}}(T=0) = 0$. Having $\mathcal{P}_{\text{eq}}(T)$, one can obtain the energy density
 196 \mathcal{E}_{eq} using $\mathcal{E}_{\text{eq}}(T) = 3\mathcal{P}_{\text{eq}}(T) + I_{\text{eq}}(T)$. In the limit $T \rightarrow \infty$, the system tends to the ideal
 197 limit as expected.³ The temperature dependence of the resulting equilibrium energy density,
 198 pressure, and speed of sound squared ($c_s^2 = \partial\mathcal{P}_{\text{eq}}/\partial\mathcal{E}_{\text{eq}}$) are shown in the two panels of Fig. 1.

199 *Method 1: Standard equation of state*

200 In the standard approach for imposing a realistic EoS in anisotropic hydrodynamics, one
 201 derives the necessary equations in the conformal limit and exploits the conformal multi-
 202 plicative factorization of the components of the energy-momentum tensor [47, 48]. With
 203 this method, one relies on the assumption of factorization even in the non-conformal (mas-
 204 sive) case. Such an approach is justified by the smallness of the corrections to factorization

³In the original parametrization presented in Ref. [70] the authors used $h_3 = 0$, however, as pointed out in Ref. [66], choosing $h_3 = 0$ gives the wrong high temperature limit.

205 in the massive case in the near-equilibrium limit [66]. For details concerning this method,
 206 we refer the reader to Refs. [54, 66]. Although this method is relatively straightforward
 207 to implement, it is only approximate since for non-conformal systems there is no longer
 208 exact multiplicative factorization of the components of the energy-momentum tensor. This
 209 introduces a theoretical uncertainty which is difficult to quantitatively estimate.

210 *Method 2: Quasiparticle equation of state*

211 Since the standard method is only approximate, one would like to find an alternative
 212 method for imposing a realistic equation of state in an anisotropic system that can be ap-
 213 plied for non-conformal systems. In order to accomplish this goal, we implement the realistic
 214 EoS detailed above by assuming that the QGP can be described as an ensemble of massive
 215 quasiparticles with temperature-dependent masses. As is well-known from the literature
 216 [9], one cannot simply substitute temperature-dependent masses into the thermodynamic
 217 functions obtained with constant masses because this would violate thermodynamic consis-
 218 tency. For an equilibrium system, one can ensure thermodynamic consistency by adding a
 219 background contribution to the energy-momentum tensor, i.e.

$$T_{\text{eq}}^{\mu\nu} = T_{\text{kinetic,eq}}^{\mu\nu} + g^{\mu\nu} B_{\text{eq}}, \quad (18)$$

220 with $B_{\text{eq}} \equiv B_{\text{eq}}(T)$ being the additional background contribution. The kinetic contribution
 221 to the energy momentum tensor is given by

$$T_{\text{eq,kinetic}}^{\mu\nu} = \int dP p^\mu p^\nu f_{\text{eq}}(x, p). \quad (19)$$

222 For an equilibrium Boltzmann gas, the number and entropy densities are unchanged,
 223 while, due to the additional background contribution, the energy density and pressure are

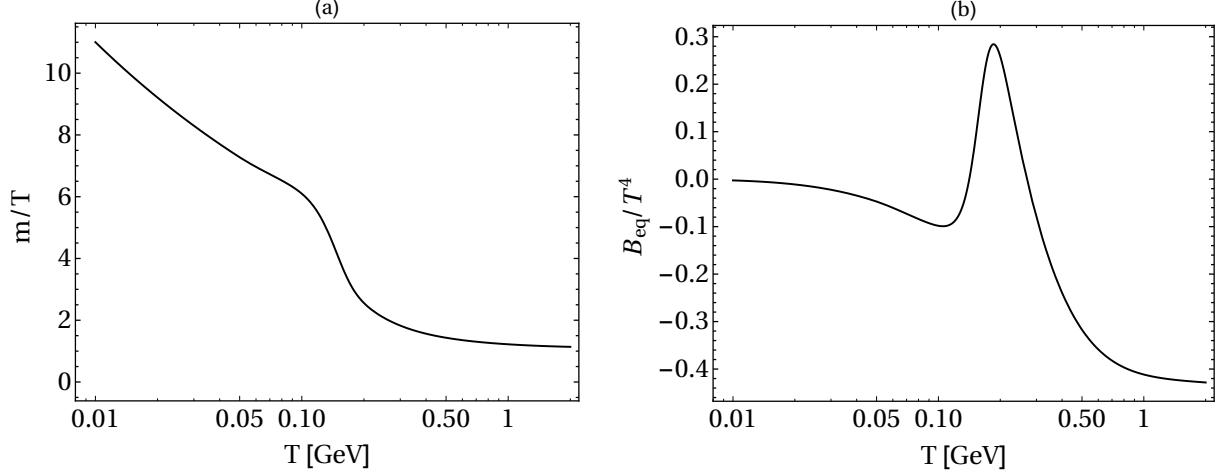


FIG. 2. In panel (a) we plot the temperature dependence of the quasiparticle mass scaled by the temperature obtained using Eq. (26). In panel (b) we plot the temperature dependence of the background term B_{eq} scaled by the temperature obtained using (25).

224 shifted by $+B_{\text{eq}}$ and $-B_{\text{eq}}$, respectively, giving

$$n_{\text{eq}}(T, m) = 4\pi \tilde{N} T^3 \hat{m}_{\text{eq}}^2 K_2(\hat{m}_{\text{eq}}), \quad (20)$$

$$\mathcal{S}_{\text{eq}}(T, m) = 4\pi \tilde{N} T^3 \hat{m}_{\text{eq}}^2 \left[4K_2(\hat{m}_{\text{eq}}) + \hat{m}_{\text{eq}} K_1(\hat{m}_{\text{eq}}) \right], \quad (21)$$

$$\mathcal{E}_{\text{eq}}(T, m) = 4\pi \tilde{N} T^4 \hat{m}_{\text{eq}}^2 \left[3K_2(\hat{m}_{\text{eq}}) + \hat{m}_{\text{eq}} K_1(\hat{m}_{\text{eq}}) \right] + B_{\text{eq}}, \quad (22)$$

$$\mathcal{P}_{\text{eq}}(T, m) = 4\pi \tilde{N} T^4 \hat{m}_{\text{eq}}^2 K_2(\hat{m}_{\text{eq}}) - B_{\text{eq}}, \quad (23)$$

225 where $\hat{m}_{\text{eq}} = m/T$ with m implicitly depending on the temperature from here on. In order
 226 to fix B_{eq} , one can require, for example, the thermodynamic identity

$$T\mathcal{S}_{\text{eq}} = \mathcal{E}_{\text{eq}} + \mathcal{P}_{\text{eq}} = T \frac{\partial \mathcal{P}_{\text{eq}}}{\partial T}, \quad (24)$$

227 be satisfied. Using Eqs. (22), (23), and (24) one obtains

$$\begin{aligned} \frac{dB_{\text{eq}}}{dT} &= -\frac{1}{2} \frac{dm^2}{dT} \int dP f_{\text{eq}}(x, p) \\ &= -4\pi \tilde{N} m^2 T K_1(\hat{m}_{\text{eq}}) \frac{dm}{dT}. \end{aligned} \quad (25)$$

228 If the temperature dependence of m is known, then Eq. (25) can be used to determine B_{eq} .

229 In order to determine m , one can use the thermodynamic identity

$$\mathcal{E}_{\text{eq}} + \mathcal{P}_{\text{eq}} = T\mathcal{S}_{\text{eq}} = 4\pi\tilde{N}T^4 \hat{m}_{\text{eq}}^3 K_3(\hat{m}_{\text{eq}}). \quad (26)$$

230 Using the lattice parameterization (16) to compute the equilibrium energy density and pres-
 231 sure, one can numerically solve for $m(T)$. In Fig. 2a, we plot the resulting solution for
 232 m/T as a function of the temperature. Once m is determined using Eq. (26), one can solve
 233 Eq. (25) subject to the boundary condition $B_{\text{eq}}(T=0) = 0$ to find $B_{\text{eq}}(T)$. We note that,
 234 using this method, one can exactly reproduce the lattice results for energy density, pressure,
 235 and entropy density. In Fig. 2b, we plot the resulting solution for the normalized quantity
 236 $B_{\text{eq}}(T)/T^4$ as a function of the temperature.

237 IV. BOLTZMANN EQUATION AND ITS MOMENTS

238 In this paper, we derive the necessary hydrodynamical equations by taking the moments
 239 of Boltzmann equation. In what follows, we specialize to the case that the collisional kernel is
 240 given by the relaxation-time approximation (RTA), however, the general methods presented
 241 here can be applied to any collisional kernel. If the particles that comprise the system have
 242 temperature-independent masses then the Boltzmann equation is of the form

$$p^\mu \partial_\mu f = -\mathcal{C}[f]. \quad (27)$$

243 The function $\mathcal{C}[f]$ at right-hand side of the equation is the collisional kernel containing all
 244 interactions involved in the dynamics. In RTA, one has

$$\mathcal{C}[f] = \frac{p^\mu u_\mu}{\tau_{\text{eq}}} (f - f_{\text{eq}}). \quad (28)$$

245 In this relation, f_{eq} denotes the equilibrium one-particle distribution function (15) and τ_{eq} is
 246 the relaxation time which can depend on spacetime but which we assume to be momentum-
 247 independent. To obtain a realistic model for τ_{eq} , which is valid for massive systems, one
 248 can relate τ_{eq} to the shear viscosity to entropy density ratio. For a massive system, one has
 249 [71, 72]

$$\eta(T) = \frac{\tau_{\text{eq}}(T)\mathcal{P}_{\text{eq}}(T)}{15} \kappa(\hat{m}_{\text{eq}}). \quad (29)$$

250 In this formula the function $\kappa(x)$ is defined as

$$\kappa(x) \equiv x^3 \left[\frac{3}{x^2} \frac{K_3(x)}{K_2(x)} - \frac{1}{x} + \frac{K_1(x)}{K_2(x)} - \frac{\pi}{2} \frac{1 - xK_0(x)L_{-1}(x) - xK_1(x)L_0(x)}{K_2(x)} \right], \quad (30)$$

251 where $K_n(x)$ are modified Bessel functions of second kind and $L_n(x)$ are modified Struve
 252 functions. Assuming that the ratio of the shear viscosity to entropy density, $\eta/\mathcal{S}_{\text{eq}} \equiv \bar{\eta}$, is
 253 held fixed during the evolution and using the thermodynamic relation $\mathcal{E}_{\text{eq}} + \mathcal{P}_{\text{eq}} = T\mathcal{S}_{\text{eq}}$ one
 254 obtains

$$\tau_{\text{eq}}(T) = \frac{15\bar{\eta}}{\kappa(\hat{m}_{\text{eq}})T} \left(1 + \frac{\mathcal{E}_{\text{eq}}(T)}{\mathcal{P}_{\text{eq}}(T)} \right). \quad (31)$$

255 Note that, in the massless limit, $m \rightarrow 0$, one has $\kappa(\hat{m}_{\text{eq}}) \rightarrow 12$, giving

$$\tau_{\text{eq}}(T) = \frac{5\eta}{4\mathcal{P}_{\text{eq}}(T)}. \quad (32)$$

256 A. Effective Boltzmann Equation

257 If the quasiparticles have a temperature-dependent mass, one has to generalize the Boltz-
 258 mann equation in order to take into account gradients in the mass. Generally, the Boltzmann
 259 equation for on-shell quasiparticles can be written as [10]

$$\left(\frac{\partial}{\partial t} + \frac{\partial E}{\partial \mathbf{p}} \cdot \frac{\partial}{\partial \mathbf{x}} - \frac{\partial E}{\partial \mathbf{x}} \cdot \frac{\partial}{\partial \mathbf{p}} \right) f(x, p) = \left(\frac{\partial f}{\partial t} \right)_{\text{coll}}, \quad (33)$$

260 where the “external force term” $-dE/d\mathbf{x}$ does not vanish in the thermal mass case since the
 261 particle energy depends on the mass and hence on the local temperature of the system. As
 262 a result, the temperature-dependence of the mass acts as an external force in the dynamics.
 263 Using the on-shell energy relation $E \equiv \sqrt{\mathbf{p}^2 + m^2}$ and defining the collisional kernel as

$$\mathcal{C}[f] \equiv -E \left(\frac{\partial f}{\partial t} \right)_{\text{coll}}, \quad (34)$$

264 in covariant form one has

$$p^\mu \partial_\mu f + \frac{1}{2} \partial_i m^2 \partial_{(p)}^i f = -\mathcal{C}[f], \quad (35)$$

265 where $p^\mu \equiv (\sqrt{\mathbf{p}^2 + m^2}, \mathbf{p})$ is the on-shell momentum four-vector, i is a spatial coordinate
 266 index, and $\partial_{(p)}^i \equiv -\partial/\partial p^i$. Note that the extra term, $(\partial_i m^2/2)\partial_{(p)}^i f$, corresponds precisely

267 to the result obtained from derivation of the Boltzmann equation using quantum field the-
 268 oretical methods [73].

269 We mention that an alternative way of deriving the effective Boltzmann equation above
 270 can be found in a recent paper of Romatschke [11]. In this paper, a general Boltzmann
 271 equation for off-shell particles (with constant mass) is first derived using the evolution of
 272 a single particle distribution function along eight-dimensional phase space geodesics, where
 273 the possibility of curved spaces is taken into account using geometrical covariant derivatives.
 274 Then, by adding a temperature-dependent background term to $T^{\mu\nu}$, temperature-dependent
 275 masses are taken into account in a way that guarantees both thermodynamic consistency in
 276 the equilibrium limit and energy-momentum conservation, in general. Finally, the on-shell
 277 version of the effective Boltzmann equation for quasiparticles with a temperature-dependent
 278 mass in a general curved space time is obtained. The flat spacetime limit of the effective
 279 Boltzmann equation derived by Romatschke is the same as Eq. (35).

280 B. Moments of Boltzmann Equation

281 If one is interested in the evolution of the bulk properties of a system, one can use low-
 282 order moments of the Boltzmann equation. By calculating moments of Boltzmann equation
 283 one obtains evolution equations for tensors of different ranks, with the first moment giving an
 284 evolution equation for the energy-momentum tensor and the second-moment describing the
 285 evolution of a rank three tensor. Taking the zeroth, first, and second moments of Boltzmann
 286 equation gives, respectively

$$\partial_\mu J^\mu = - \int dP \mathcal{C}[f], \quad (36)$$

$$\partial_\mu T^{\mu\nu} = - \int dP p^\nu \mathcal{C}[f], \quad (37)$$

$$\partial_\mu \mathcal{I}^{\mu\nu\lambda} - J^{(\nu} \partial^{\lambda)} m^2 = - \int dP p^\nu p^\lambda \mathcal{C}[f], \quad (38)$$

287 where the particle four-current J^μ , energy-momentum tensor $T^{\mu\nu}$, and the rank-three tensor
 288 $\mathcal{I}^{\mu\nu\lambda}$ are given by

$$J^\mu \equiv \int dP p^\mu f(x, p), \quad (39)$$

$$T^{\mu\nu} \equiv \int dP p^\mu p^\nu f(x, p) + Bg^{\mu\nu}, \quad (40)$$

$$\mathcal{I}^{\mu\nu\lambda} \equiv \int dP p^\mu p^\nu p^\lambda f(x, p). \quad (41)$$

289 We note that we have introduced the non-equilibrium background field $B \equiv B(\boldsymbol{\alpha}, \lambda)$, which
 290 is the analogue of the equilibrium background B_{eq} in order to guarantee that the correct
 291 equilibrium limit of $T^{\mu\nu}$ is obtained. In the process of the derivation one finds that, in order
 292 to write the energy momentum conservation in the form given in Eq. (37), there must be a
 293 differential equation relating B and the thermal mass

$$\partial_\mu B = -\frac{1}{2}\partial_\mu m^2 \int dP f(x, p). \quad (42)$$

294 In practice, one can use (42) to write the derivative of B with respect to any variable in
 295 terms of the derivative of the thermal mass times the E^{-1} moment of the non-equilibrium
 296 distribution function.

297 V. BULK VARIABLES

298 In this section, bulk variables, i.e. number density, energy density, and the pressures, are
 299 calculated by taking the projections of J^μ and $T^{\mu\nu}$.

300 A. Particle current 4-vector

301 The particle current four-vector $J^\mu \equiv (n, \mathbf{J})$ is defined in Eq. (39). One can expand J^μ
 302 using the basis vectors as

$$J^\mu = nu^\mu + J_x X^\mu + J_y Y^\mu + J_z Z^\mu. \quad (43)$$

303 Using Eqs. (13) and (39) one has

$$J^\mu = (n, \mathbf{0}) = nu^\mu, \quad (44)$$

304 where $n = \alpha n_{\text{eq}}(\lambda, m)$ and $\alpha \equiv \alpha_x \alpha_y \alpha_z$.

305 B. Energy-Momentum Tensor

306 The energy-momentum tensor $T^{\mu\nu}$ is defined in Eq. (40). Expanding it using the basis
307 vectors one obtains

$$T^{\mu\nu} = \mathcal{E}u^\mu u^\nu + \mathcal{P}_x X^\mu X^\nu + \mathcal{P}_y Y^\mu Y^\nu + \mathcal{P}_z Z^\mu Z^\nu. \quad (45)$$

308 Using Eqs. (13), (40), and (45) and taking projections of $T^{\mu\nu}$ one can obtain the energy
309 density and the components of pressure

$$\begin{aligned} \mathcal{E} &= \mathcal{H}_3(\boldsymbol{\alpha}, \hat{m}) \lambda^4 + B, \\ \mathcal{P}_x &= \mathcal{H}_{3x}(\boldsymbol{\alpha}, \hat{m}) \lambda^4 - B, \\ \mathcal{P}_y &= \mathcal{H}_{3y}(\boldsymbol{\alpha}, \hat{m}) \lambda^4 - B, \\ \mathcal{P}_z &= \mathcal{H}_{3L}(\boldsymbol{\alpha}, \hat{m}) \lambda^4 - B, \end{aligned} \quad (46)$$

310 where $\hat{m} \equiv m/\lambda$. In the transversally-symmetric case one has $\mathcal{P}_T \equiv \mathcal{P}_x = \mathcal{P}_y$ and $\mathcal{P}_L \equiv \mathcal{P}_z$
311 and Eq. (45) simplifies to

$$T^{\mu\nu} = (\mathcal{E} + \mathcal{P}_T) u^\mu u^\nu - \mathcal{P}_T g^{\mu\nu} + (\mathcal{P}_L - \mathcal{P}_T) Z^\mu Z^\nu, \quad (47)$$

312 where

$$\begin{aligned} \mathcal{E} &= \tilde{\mathcal{H}}_3(\boldsymbol{\alpha}, \hat{m}) \lambda^4 + B, \\ \mathcal{P}_T &= \tilde{\mathcal{H}}_{3T}(\boldsymbol{\alpha}, \hat{m}) \lambda^4 - B, \\ \mathcal{P}_L &= \tilde{\mathcal{H}}_{3L}(\boldsymbol{\alpha}, \hat{m}) \lambda^4 - B. \end{aligned} \quad (48)$$

313 The various \mathcal{H} -functions appearing above are defined in App. B 1.

314 **VI. DYNAMICAL EQUATIONS**

315 In order to obtain the dynamical equations from Eqs. (36)-(38), one needs the tensor de-
 316 composition of J^μ , $T^{\mu\nu}$, and $\mathcal{I}^{\mu\nu\lambda}$ using the basis vectors. Herein the general 3+1d equations
 317 for a system with temperature-dependent masses are obtained in the RTA. We then simplify
 318 to the case of 0+1d transversally-symmetric case by the taking necessary limits. In what
 319 follows, the convective derivatives D_α and divergences θ_α , with $\alpha \in \{u, x, y, z\}$, are defined
 320 in App. A.

321 **A. Zeroth moment**

322 The evolution equation for the particle four-current (36) in the RTA is

$$\partial_\mu J^\mu = \frac{1}{\tau_{\text{eq}}}(n_{\text{eq}} - n). \quad (49)$$

323 Using Eq. (44) one has

$$D_u n + n\theta_u = \frac{1}{\tau_{\text{eq}}}(n_{\text{eq}} - n). \quad (50)$$

324 In the case of 0+1d, this simplifies to

$$\partial_\tau n + \frac{n}{\tau} = \frac{1}{\tau_{\text{eq}}}(n_{\text{eq}} - n). \quad (51)$$

325 **B. First Moment**

326 The conservation of energy and momentum is enforced by $\partial_\mu T^{\mu\nu} = 0$. This requires that
 327 both the left and right hand sides of Eq. (37) vanish. The vanishing of the right-hand side
 328 of this equation results in a constraint equation that can be used to write T in terms of the
 329 non-equilibrium microscopic parameters α and λ . Using (13), (15), and (28) one obtains
 330 $\mathcal{E}_{\text{kinetic}} = \mathcal{E}_{\text{eq,kinetic}}$, or more explicitly

$$\tilde{\mathcal{H}}_3 \lambda^4 = \tilde{\mathcal{H}}_{3,\text{eq}} T^4. \quad (52)$$

331 Turning to the left hand side, using Eq. (45) and taking U -, X -, Y -, and Z -projections,

332 one obtains four independent equations

$$\begin{aligned}
D_u \mathcal{E} + \mathcal{E} \theta_u + \mathcal{P}_x u_\mu D_x X^\mu + \mathcal{P}_y u_\mu D_y Y^\mu + \mathcal{P}_z u_\mu D_z Z^\mu &= 0, \\
D_x \mathcal{P}_x + \mathcal{P}_x \theta_x - \mathcal{E} X_\mu D_u u^\mu - \mathcal{P}_y X_\mu D_y Y^\mu - \mathcal{P}_z X_\mu D_z Z^\mu &= 0, \\
D_y \mathcal{P}_y + \mathcal{P}_y \theta_y - \mathcal{E} Y_\mu D_u u^\mu - \mathcal{P}_x Y_\mu D_x X^\mu - \mathcal{P}_z Y_\mu D_z Z^\mu &= 0, \\
D_z \mathcal{P}_z + \mathcal{P}_z \theta_z - \mathcal{E} Z_\mu D_u u^\mu - \mathcal{P}_x Z_\mu D_x X^\mu - \mathcal{P}_y Z_\mu D_y Y^\mu &= 0.
\end{aligned} \tag{53}$$

333 In the 0+1d case, using $\mathcal{P}_T \equiv \mathcal{P}_x = \mathcal{P}_y$ and $\mathcal{P}_L \equiv \mathcal{P}_z$ and taking the appropriate limits, as
334 explained in App. A, one can simplify Eqs. (53) to

$$\partial_\tau \mathcal{E} = -\frac{\mathcal{E} + \mathcal{P}_L}{\tau}, \tag{54}$$

$$\partial_r \mathcal{P}_T = \partial_\phi \mathcal{P}_T = \partial_\zeta \mathcal{P}_L = 0. \tag{55}$$

335 Eqs. (55) are consequences of boost invariance and transverse homogeneity in the 0+1d case
336 and, as a result, the only independent dynamical equation is Eq. (54).

337 C. Second moment

338 The second moment of Boltzmann equation in the RTA is

$$\partial_\mu \mathcal{I}^{\mu\nu\lambda} - J^{(\nu} \partial^{\lambda)} m^2 = \frac{1}{\tau_{\text{eq}}} (u_\mu \mathcal{I}_{\text{eq}}^{\mu\nu\lambda} - u_\mu \mathcal{I}^{\mu\nu\lambda}), \tag{56}$$

339 where $\mathcal{I}_{\text{eq}}^{\mu\nu\lambda}$ can be obtained from Eq. (41) by taking $f \rightarrow f_{\text{eq}}$. For a distribution function
340 of the form specified in Eq. (13), the only non-vanishing terms in Eq. (41) are those with
341 an even number of similar spatial index. As a result, one can expand $\mathcal{I}^{\mu\nu\lambda}$ over the basis
342 vectors as

$$\begin{aligned}
\mathcal{I} &= \mathcal{I}_u [u \otimes u \otimes u] \\
&+ \mathcal{I}_x [u \otimes X \otimes X + X \otimes u \otimes X + X \otimes X \otimes u] \\
&+ \mathcal{I}_y [u \otimes Y \otimes Y + Y \otimes u \otimes Y + Y \otimes Y \otimes u] \\
&+ \mathcal{I}_z [u \otimes Z \otimes Z + Z \otimes u \otimes Z + Z \otimes Z \otimes u].
\end{aligned} \tag{57}$$

343 Evaluating the necessary integrals using the distribution function (13), one finds

$$\mathcal{I}_u = \left(\sum_i \alpha_i^2 \right) \alpha \mathcal{I}_{\text{eq}}(\lambda, m) + \alpha m^2 n_{\text{eq}}(\lambda, m), \quad (58)$$

$$\mathcal{I}_i = \alpha \alpha_i^2 \mathcal{I}_{\text{eq}}(\lambda, m), \quad (59)$$

344 where

$$\mathcal{I}_{\text{eq}}(\lambda, m) = 4\pi \tilde{N} \lambda^5 \hat{m}^3 K_3(\hat{m}). \quad (60)$$

345 Note that, in general, one has $\mathcal{I}_u - \sum_i \mathcal{I}_i = \alpha m^2 n_{\text{eq}}(\lambda, m)$ and $\lim_{m \rightarrow 0} \mathcal{I}_u = \sum_i \mathcal{I}_i$. Expanding

346 Eq. (56) and taking its uu -, XX -, YY -, and ZZ -projections gives

$$D_u \mathcal{I}_u + \mathcal{I}_u \theta_u + 2\mathcal{I}_x u_\mu D_x X^\mu + 2\mathcal{I}_y u_\mu D_y Y^\mu + 2\mathcal{I}_z u_\mu D_z Z^\mu - n D_u m^2 = \frac{1}{\tau_{\text{eq}}} (\mathcal{I}_{u,\text{eq}} - \mathcal{I}_u), \quad (61)$$

$$D_u \mathcal{I}_x + \mathcal{I}_x (\theta_u + 2u_\mu D_x X^\mu) = \frac{1}{\tau_{\text{eq}}} (\mathcal{I}_{\text{eq}} - \mathcal{I}_x), \quad (62)$$

$$D_u \mathcal{I}_y + \mathcal{I}_y (\theta_u + 2u_\mu D_y Y^\mu) = \frac{1}{\tau_{\text{eq}}} (\mathcal{I}_{\text{eq}} - \mathcal{I}_y), \quad (63)$$

$$D_u \mathcal{I}_z + \mathcal{I}_z (\theta_u + 2u_\mu D_z Z^\mu) = \frac{1}{\tau_{\text{eq}}} (\mathcal{I}_{\text{eq}} - \mathcal{I}_z). \quad (64)$$

347 Also, taking uX -, uY -, and uZ -projections one can find

$$D_x \mathcal{I}_x + \mathcal{I}_x \theta_x + (\mathcal{I}_x + \mathcal{I}_u) u_\mu D_u X^\mu - \mathcal{I}_y X_\mu D_y Y^\mu - \mathcal{I}_z X_\mu D_z Z^\mu - \frac{1}{2} n D_x m^2 = 0, \quad (65)$$

$$D_y \mathcal{I}_y + \mathcal{I}_y \theta_y + (\mathcal{I}_y + \mathcal{I}_u) u_\mu D_u Y^\mu - \mathcal{I}_x Y_\mu D_x X^\mu - \mathcal{I}_z Y_\mu D_z Z^\mu - \frac{1}{2} n D_y m^2 = 0, \quad (66)$$

$$D_z \mathcal{I}_z + \mathcal{I}_z \theta_z + (\mathcal{I}_z + \mathcal{I}_u) u_\mu D_u Z^\mu - \mathcal{I}_x Z_\mu D_x X^\mu - \mathcal{I}_y Z_\mu D_y Y^\mu - \frac{1}{2} n D_z m^2 = 0, \quad (67)$$

348 and finally projecting with XY , XZ , and YZ gives

$$\mathcal{I}_x (Y_\mu D_u X^\mu + Y_\mu D_x u^\mu) + \mathcal{I}_y (X_\mu D_u Y^\mu + X_\mu D_y u^\mu) = 0, \quad (68)$$

$$\mathcal{I}_x (Z_\mu D_u X^\mu + Z_\mu D_x u^\mu) + \mathcal{I}_z (X_\mu D_u Z^\mu + X_\mu D_z u^\mu) = 0, \quad (69)$$

$$\mathcal{I}_y (Z_\mu D_u Y^\mu + Z_\mu D_y u^\mu) + \mathcal{I}_z (Y_\mu D_u Z^\mu + Y_\mu D_z u^\mu) = 0. \quad (70)$$

349 It can be shown that Eq. (61) is not independent. One can subtract the sum of Eqs. (62)-

350 (64) from it to obtain

$$m^2 (D_u n + n \theta_u) = \frac{m^2}{\tau_{\text{eq}}} (n_{\text{eq}} - n). \quad (71)$$

351 This equation is the same as Eq. (50) for non-vanishing mass. In the 0+1d case, one has
 352 $\mathcal{I}_x = \mathcal{I}_y$ and Eqs. (62)-(64) simplify to

$$D_u \log \mathcal{I}_x + \frac{1}{\tau} = \frac{1}{\tau_{\text{eq}}} \left(\frac{\mathcal{I}_{\text{eq}}}{\mathcal{I}_x} - 1 \right), \quad (72)$$

$$D_u \log \mathcal{I}_z + \frac{3}{\tau} = \frac{1}{\tau_{\text{eq}}} \left(\frac{\mathcal{I}_{\text{eq}}}{\mathcal{I}_z} - 1 \right). \quad (73)$$

353 Finally, we note that Eqs. (65)-(70) are trivially satisfied in the 0+1d case.

354 **D. Selection of relevant equations of motion**

355 For the 0+1d case, we need four equations for the four independent parameters, $\lambda, T, \alpha_x, \alpha_z$.
 356 Using the equations derived thus far up to the second moment of Boltzmann equation, we
 357 have five independent equations. Herein, we use the equations obtained solely from the first
 358 and second moments of the Boltzmann equation which give Eqs. (52), (54), (72), and (73).⁴

359 **VII. 0+1D DYNAMICAL EQUATIONS**

360 In this section, we present the dynamical equations for the “quasiparticle EoS” and the
 361 “standard EoS” cases. For simplicity, we present only the 0+1d case herein. We postpone
 362 the 3+1d numerical comparisons to a future work.

363 **A. Quasiparticle equation of state**

364 One potential complication encountered when using temperature-dependent masses is
 365 that the first moment equation will involve the background contribution B and its proper-
 366 time derivative, since on the left-hand side of (54) one has the total energy density which
 367 includes the background contribution. In practice, however, all derivatives of B can be
 368 written in terms of derivatives of m using Eq. (42). For the 0+1d case, we only need the
 369 proper-time derivative of B . Taking the distribution function to be of the form (13) and
 370 using Eq. (42) one obtains

$$\partial_\tau B = -\frac{\lambda^2}{2} \tilde{\mathcal{H}}_{3B}(\boldsymbol{\alpha}, \hat{m}) \partial_\tau m^2. \quad (74)$$

⁴For the “quasiparticle EoS” case one obtains quite similar results if one instead uses the equation obtained from the zeroth-moment (51); however, in the “standard EoS” case, one finds that using the zeroth moment equation (51) results in solutions that do not approach the isotropic equilibrium limit at late times.

371 In this way, all proper-time derivatives of B necessary for the evolution equations can be
372 obtained from derivatives of the thermal mass and knowledge of the non-equilibrium mi-
373 croscopic parameters which enter the $\tilde{\mathcal{H}}_{3B}$ function. However, in order to obtain the total
374 energy density or pressures one needs to know B itself. Our procedure will be to integrate
375 the dynamical equations to a very late proper time τ_f when the system is close to equilib-
376 rium and then integrate Eq. (74) backwards in time from τ_f to the initial time τ_0 subject to
377 the boundary condition that $B(\tau_f) = B_{\text{eq}}(T(\tau_f))$.

378 Using Eqs. (48), (59), and (60) one can expand (54), (72), and (73) to obtain

$$4\tilde{\mathcal{H}}_3\partial_\tau \log \lambda + \tilde{\Omega}_m\partial_\tau \log \hat{m} + \tilde{\Omega}_L\partial_\tau \log \alpha_z + \tilde{\Omega}_T\partial_\tau \log \alpha_x^2 + \frac{\partial_\tau B}{\lambda^4} + \frac{\tilde{\Omega}_L}{\tau} = 0, \quad (75)$$

$$4\partial_\tau \log \alpha_x + \partial_\tau \log \alpha_z + 5\partial_\tau \log \lambda + \partial_\tau \log(\hat{m}^3 K_3(\hat{m})) + \frac{1}{\tau} \\ = \frac{1}{\tau_{\text{eq}}} \left[\frac{1}{\alpha_x^4 \alpha_z} \left(\frac{T}{\lambda}\right)^2 \frac{K_3(\hat{m}_{\text{eq}})}{K_3(\hat{m})} - 1 \right], \quad (76)$$

$$2\partial_\tau \log \alpha_x + 3\partial_\tau \log \alpha_z + 5\partial_\tau \log \lambda + \partial_\tau \log(\hat{m}^3 K_3(\hat{m})) + \frac{3}{\tau} \\ = \frac{1}{\tau_{\text{eq}}} \left[\frac{1}{\alpha_x^2 \alpha_z^3} \left(\frac{T}{\lambda}\right)^2 \frac{K_3(\hat{m}_{\text{eq}})}{K_3(\hat{m})} - 1 \right], \quad (77)$$

379 where $\tilde{\Omega}_T$, $\tilde{\Omega}_L$, and $\tilde{\Omega}_m$ are defined in App. B1.

380 One can perform some algebra to change the matching condition (52) into a differential
381 equation which is more convenient to solve since we then only have to solve a system of
382 coupled ordinary differential equations. Taking a derivative of Eq. (52) with respect to τ
383 and using Eq. (54), one obtains

$$4\tilde{\mathcal{H}}_{3,\text{eq}}\partial_\tau \log T + \tilde{\Omega}_{m,\text{eq}}\partial_\tau \log \hat{m}_{\text{eq}} + \frac{\tilde{\Omega}_L}{\tau} \left(\frac{\lambda}{T}\right)^4 + \frac{\partial_\tau B}{T^4} = 0. \quad (78)$$

384 In all equations above one can use Eq. (31) for τ_{eq} .

385 B. Standard equation of state

386 We now present the details of our implementation of the “standard EoS” method. In this
387 case, one takes the particles to be massless, $m \rightarrow 0$, and hence $B \rightarrow 0$. For the massless

388 transversally-symmetric case, Eqs. (48) become

$$\begin{aligned}
\mathcal{E} &= \bar{\mathcal{H}}_3(\boldsymbol{\alpha}) \lambda^4, \\
\mathcal{P}_T &= \bar{\mathcal{H}}_{3T}(\boldsymbol{\alpha}) \lambda^4, \\
\mathcal{P}_L &= \bar{\mathcal{H}}_{3L}(\boldsymbol{\alpha}) \lambda^4,
\end{aligned} \tag{79}$$

389 where all \mathcal{H} -functions are defined in App. B 2. As we can see from the above equations, there
390 is a multiplicative factorization of the energy density and pressures into a function that only
391 depends on the anisotropy parameters and a function that only depends on the scale λ .
392 For a massless conformal Boltzmann gas, one has $\mathcal{E}_{\text{eq}}(T) = 24\pi\tilde{N}T^4$ and $\mathcal{P}_{\text{eq}}(T) = 8\pi\tilde{N}T^4$.
393 Using these relations, one can rewrite Eqs. (79) in terms of the equilibrium thermodynamic
394 functions

$$\begin{aligned}
\mathcal{E} &= \frac{\mathcal{E}_{\text{eq}}(\lambda)}{2} \alpha_x^4 \bar{\mathcal{H}}_2\left(\frac{\alpha_z}{\alpha_x}\right), \\
\mathcal{P}_T &= \frac{3\mathcal{P}_{\text{eq}}(\lambda)}{4} \alpha_x^4 \bar{\mathcal{H}}_{2T}\left(\frac{\alpha_z}{\alpha_x}\right), \\
\mathcal{P}_L &= \frac{3\mathcal{P}_{\text{eq}}(\lambda)}{2} \alpha_x^4 \bar{\mathcal{H}}_{2L}\left(\frac{\alpha_z}{\alpha_x}\right).
\end{aligned} \tag{80}$$

395 These formulas suggest that, in order to impose a realistic EoS, one only has to replace
396 $\mathcal{E}_{\text{eq}}(\lambda)$ and $\mathcal{P}_{\text{eq}}(\lambda)$ by the results obtained from lattice QCD calculations.

397 In order to obtain the necessary dynamical equations, one has to take the limit $m \rightarrow 0$
398 of the equations obtained from the moments of the Boltzmann equation and substitute \mathcal{E}
399 and $\mathcal{P}_{T,L}$ from Eq. (80). For the first moment equation, starting from Eq. (54) and using
400 Eq. (80) one obtains

$$\partial_\tau \log \mathcal{E}_{\text{eq}}(\lambda) + (1 + \chi) \partial_\tau \log \alpha_z + (3 - \chi) \partial_\tau \log \alpha_x = -\frac{1}{\tau} - \frac{3\mathcal{P}_{\text{eq}}(\lambda)}{\tau \mathcal{E}_{\text{eq}}(\lambda)} \chi, \tag{81}$$

401 with $\chi \equiv \bar{\mathcal{H}}_{2L}/\bar{\mathcal{H}}_2$. Taking the limit $m \rightarrow 0$ and $B \rightarrow 0$ of the second-moment equations
402 (76) and (77), one obtains

$$4\partial_\tau \log \alpha_x + \partial_\tau \log \alpha_z + 5\partial_\tau \log \lambda + \frac{1}{\tau} = \frac{1}{\tau_{\text{eq}}} \left[\left(\frac{T}{\lambda}\right)^5 \frac{1}{\alpha_x^4 \alpha_z} - 1 \right], \tag{82}$$

$$2\partial_\tau \log \alpha_x + 3\partial_\tau \log \alpha_z + 5\partial_\tau \log \lambda + \frac{3}{\tau} = \frac{1}{\tau_{\text{eq}}} \left[\left(\frac{T}{\lambda}\right)^5 \frac{1}{\alpha_x^2 \alpha_z^3} - 1 \right]. \tag{83}$$

403 For the matching relation which gives T in terms of the microscopic parameters, one can
 404 use $\mathcal{E}(\lambda) = \mathcal{E}_{\text{eq}}(T)$ and Eq. (81) to find

$$\partial_\tau \log \mathcal{E}_{\text{eq}}(T) = -\frac{1}{\tau} - \frac{3\mathcal{P}_{\text{eq}}(\lambda)}{\tau \mathcal{E}_{\text{eq}}(\lambda)} \chi. \quad (84)$$

405 In all equations above one can use Eq. (32) for τ_{eq} .

406 VIII. RESULTS

407 In this section, we present the results of numerically integrating the dynamical equations
 408 using the “standard EoS” and the “quasiparticle EoS” methods. In both cases, we specialize
 409 to the 0+1d case. We take the initial proper time to be $\tau_0 = 0.25$ fm/c and the final time to
 410 be $\tau_f = 500$ fm/c. In all cases, the initial temperature is taken to be $T_0 = 600$ MeV which
 411 is appropriate for LHC heavy-ion collisions at $\sqrt{s_{\text{NN}}} = 2.76$ TeV. The final time used here is
 412 very long compared to the timescales relevant for heavy-ion collisions, but we are interested
 413 in the late-time approach to isotropic thermal equilibrium in both approaches. Additionally,
 414 as mentioned previously, in order to determine $B(\tau)$, we solve the the differential equation
 415 (74) by evolving it backwards in proper time subject to a boundary condition that $B(\tau_f) =$
 416 $B_{\text{eq}}(T(\tau_f))$ and, consequently, we should evolve the system to a late proper-time at which
 417 the system is close to isotropic thermal equilibrium.

418 Before proceedings to our results, we need to define one quantity which has yet to be
 419 defined, namely the bulk correction to the pressure. In viscous hydrodynamics, the energy-
 420 momentum tensor is expressed generally as

$$T^{\mu\nu} = \mathcal{E}_{\text{eq}} u^\mu u^\nu - (\mathcal{P}_{\text{eq}} + \Pi) \Delta^{\mu\nu} + \pi^{\mu\nu}, \quad (85)$$

421 where $\mathcal{E}_{\text{eq}} = \mathcal{E}_{\text{eq}}(T)$ and $\mathcal{P}_{\text{eq}} = \mathcal{P}_{\text{eq}}(T)$ are the equilibrium energy density and pressure
 422 evaluated at the effective temperature. In the definition above, $\pi^{\mu\nu}$ is the shear tensor
 423 and Π is the (isotropic) bulk correction. Since $\pi^{\mu\nu}$ is a traceless tensor, $\pi^\mu_\mu = 0$, which is
 424 transverse to the fluid four-velocity, $u_\mu \pi^{\mu\nu} = 0$, one finds that the bulk correction can be
 425 computed from

$$\Pi = -\frac{1}{3} \Delta_{\mu\nu} T^{\mu\nu} - \mathcal{P}_{\text{eq}} = \frac{1}{3} (\mathcal{P}_L + 2\mathcal{P}_T) - \mathcal{P}_{\text{eq}}. \quad (86)$$

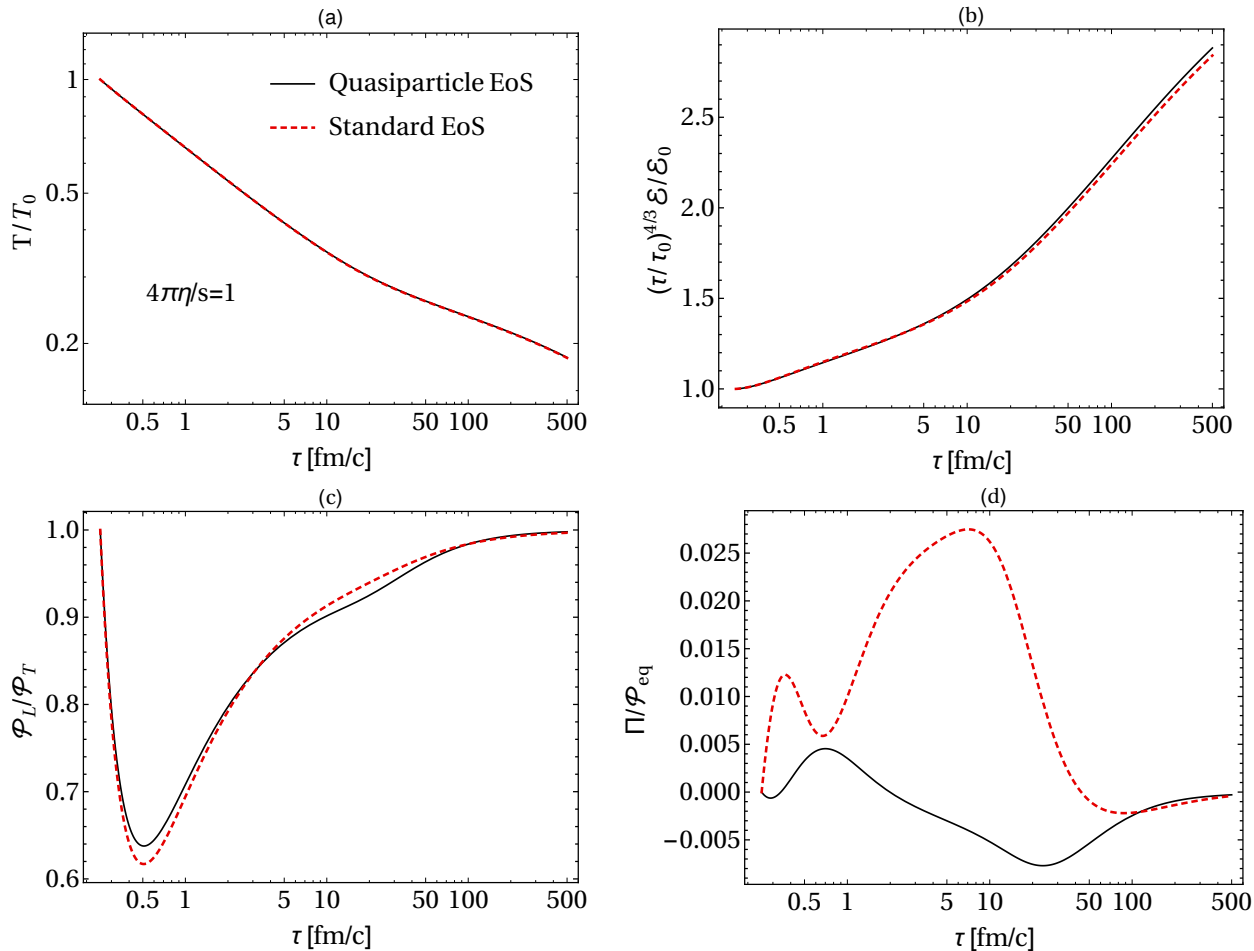


FIG. 3. The four panels show: (a) the effective temperature scaled by T_0 , (b) $(\tau/\tau_0)^{4/3}$ times the energy density scaled by the initial energy density, \mathcal{E}_0 , (c) the pressure anisotropy, and (d) the bulk correction to the pressure scaled by \mathcal{P}_{eq} . For this figure we took $4\pi\eta/s = 1$.

426 For the case of a temperature-dependent mass, one can use Eqs. (23) and (48). For the
 427 massless case, one can use Eqs. (17) and (80).

428 Numerical results

429 We now turn to our numerical results. In all plots, we compare the two methods for
 430 implementing the EoS in anisotropic hydrodynamics. For the curves labeled “Quasiparticle
 431 EoS”, we solve the dynamical equations specified in Sec. VII A and for the “Standard EoS”,
 432 we solve those in Sec. VII B. For purposes of the comparison, we match physical quantities
 433 rather than the microscopic parameters at τ_0 . In practice, this means that we specify an
 434 initial temperature T_0 , an initial momentum-space anisotropy quantified by $\mathcal{P}_{L,0}/\mathcal{P}_{T,0}$, and

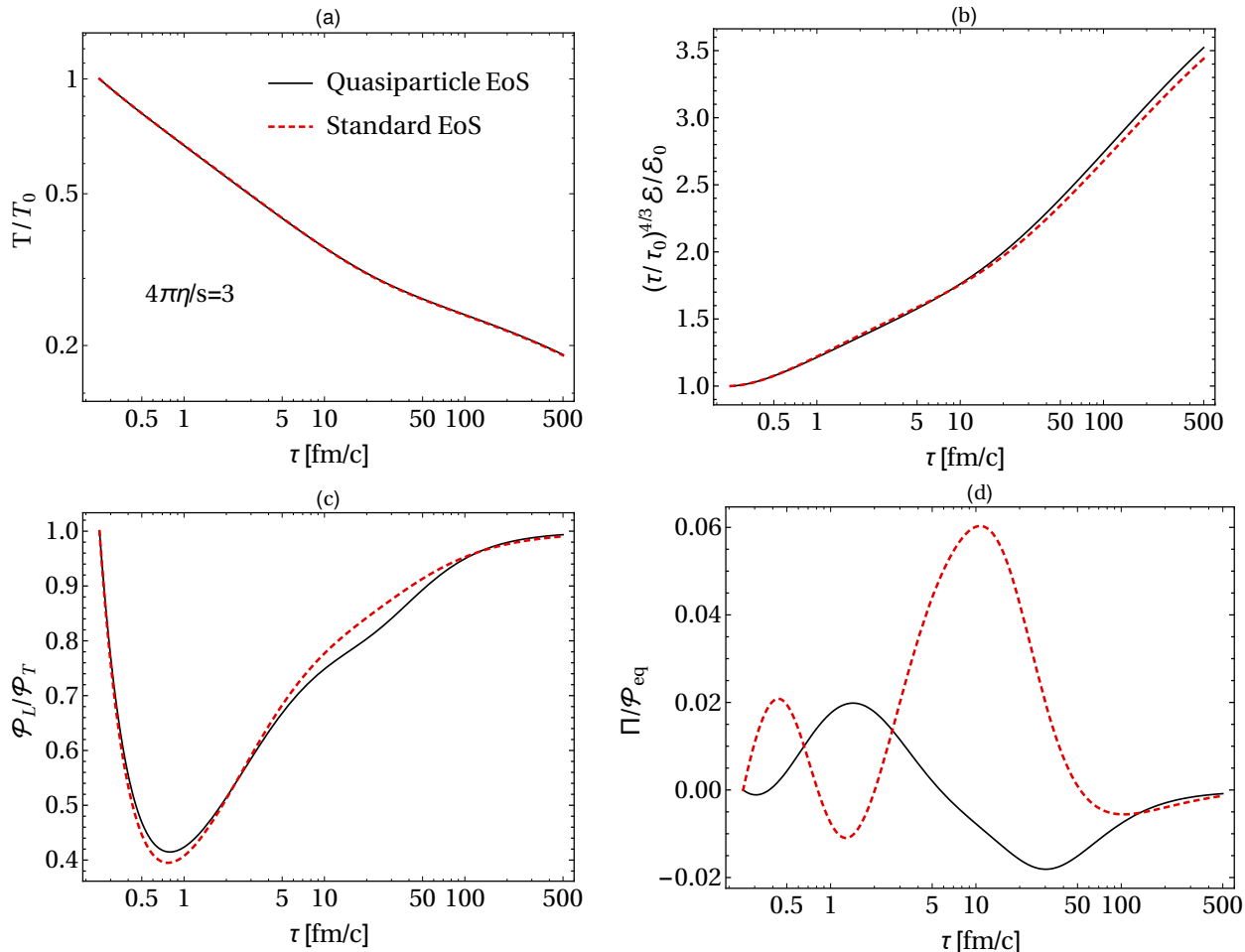


FIG. 4. Same as Fig. 3 except here we take $4\pi\eta/s = 3$.

435 an initial bulk correction, Π_0 . In all results figures, we present four panels which correspond
 436 to: (a) the effective temperature scaled by T_0 , (b) $(\tau/\tau_0)^{4/3}$ times the energy density scaled
 437 by \mathcal{E}_0 , (c) the LRF pressure anisotropy, and (d) the bulk correction scaled by the equilibrium
 438 pressure, Π/\mathcal{P}_{eq} .

439 In Figs. 3 - 5 we present our results for the case of isotropic initial conditions. In all
 440 panels, the microscopic parameters were adjusted to achieve $\mathcal{P}_{L,0}/\mathcal{P}_{T,0} = 1$ and $\Pi_0 = 0$.
 441 From panel (a) of this set of figures, we see that there is excellent agreement between
 442 the effective temperature predicted by each method for implementing the EoS. In practice,
 443 we found that, for all initial conditions we considered, the maximum difference between
 444 the effective temperature obtained using the two approaches was less than on the order of
 445 1%. To further explore the differences in the “first order” quantities, in panel (b) we have
 446 multiplied the scaled energy density by a factor of $(\tau/\tau_0)^{4/3}$. If the system behaved as an

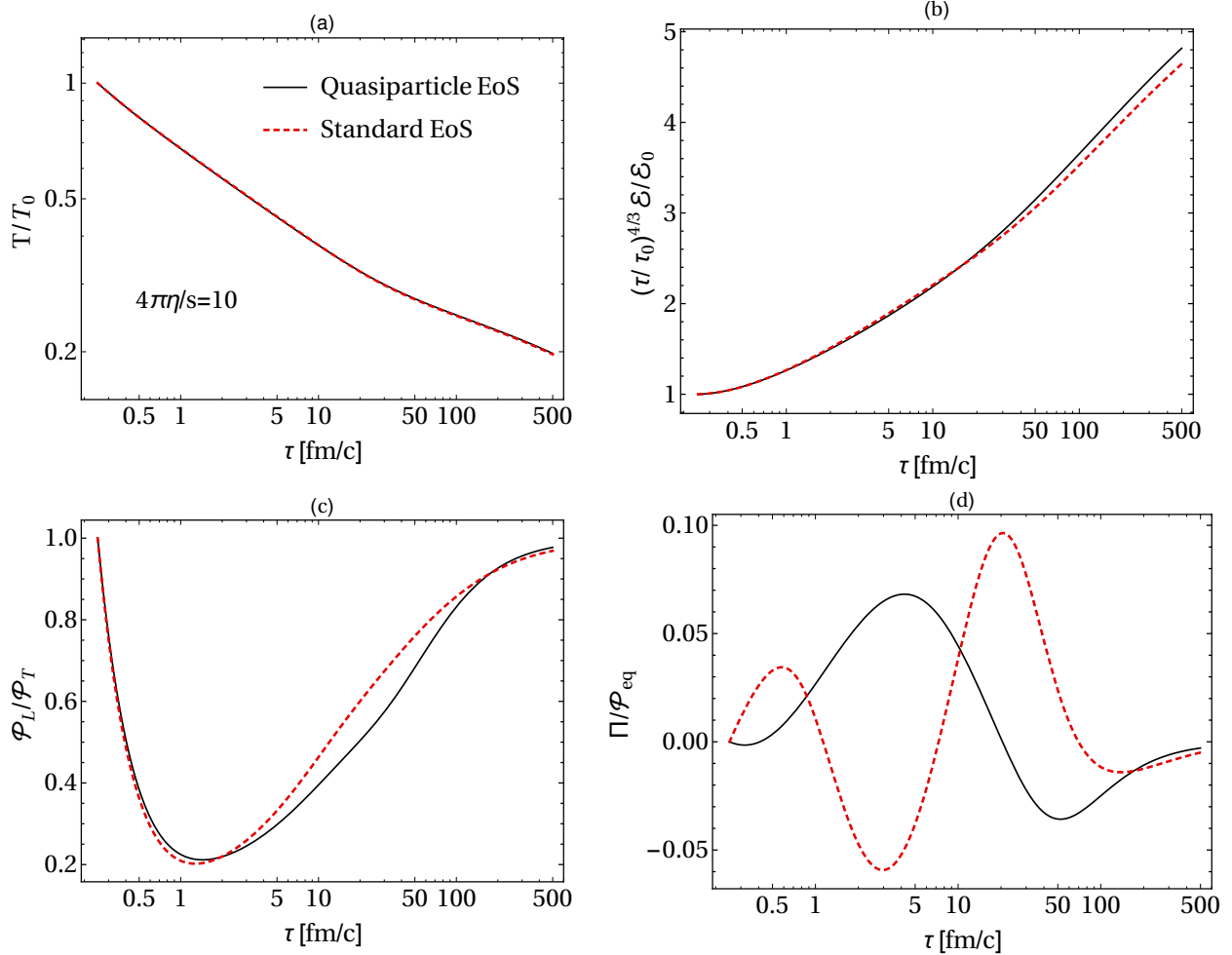


FIG. 5. Same as Fig. 3 except here we take $4\pi\eta/s = 10$.

447 ideal gas undergoing boost-invariant expansion in ideal hydrodynamics, then at late times
 448 this quantity should approach unity. Any late-time deviations from unity are indicative of
 449 the corrections to ideal Bjorken scaling. As we can see from panel (b) of Figs. 3 - 5, the
 450 energy density evolution obtained using the two approaches is quite close, with the largest
 451 difference between the two approaches being approximately 4%.

452 Considering panel (c) of Figs. 3 - 5, we see that there are larger differences in the pressure
 453 anisotropy predicted by the two approaches. For this quantity, we see differences as large
 454 as 20%, however, the behavior of the pressure anisotropy is qualitatively the same overall.
 455 Finally, we turn to panel (d) of Figs. 3 - 5 which shows the bulk correction scaled by
 456 the equilibrium pressure. As we see from these panels, there is a qualitative difference in
 457 the temporal evolution of the bulk correction when comparing the two approaches. At late
 458 times, however, both approaches seem to converge to the same asymptotic limiting behavior.

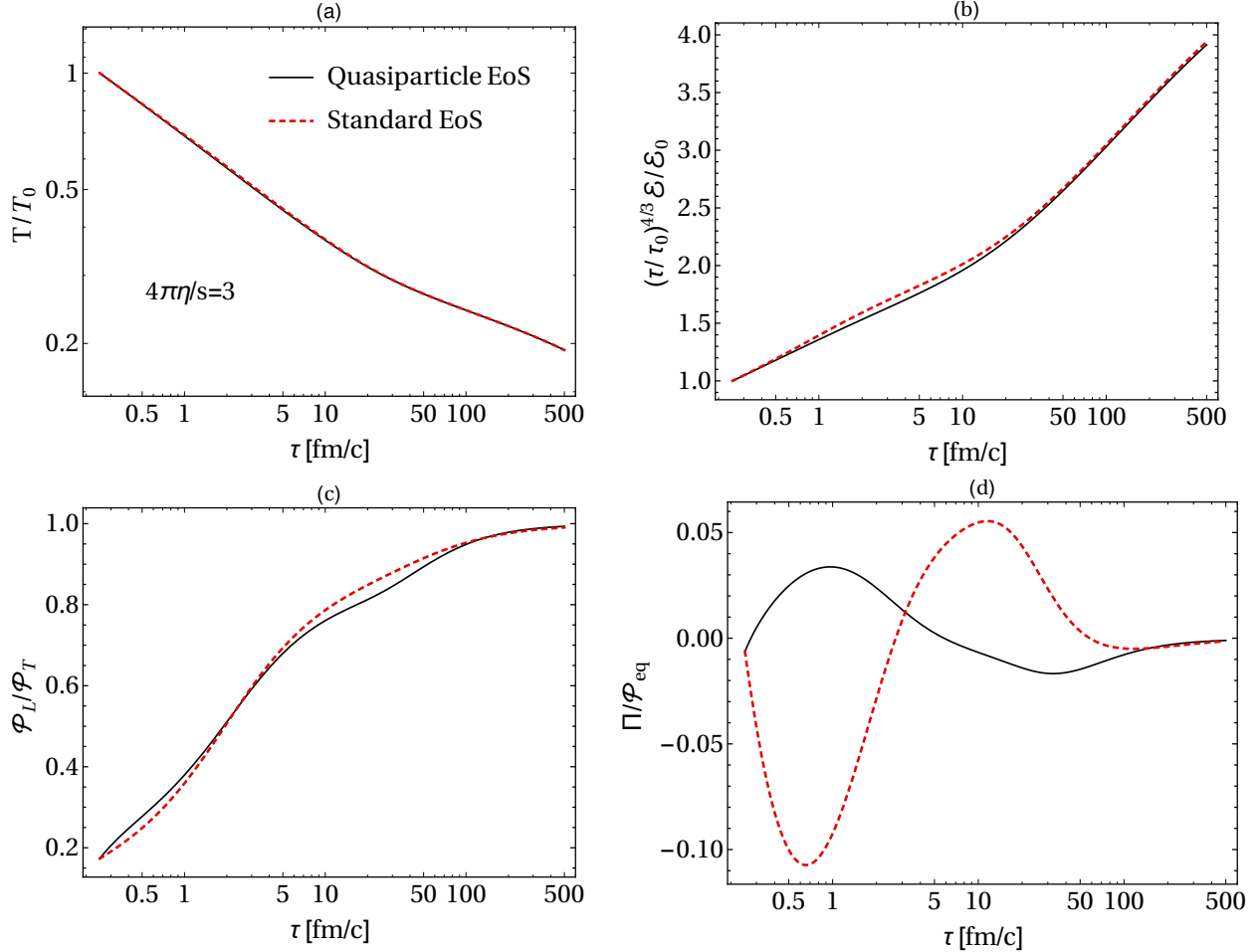


FIG. 6. Same as Fig. 4 except here we take anisotropic initial conditions.

459 Note that the differences in the pressure anisotropy and bulk correction are already self-
 460 consistently taken into account in the evolution of the temperature/energy density. In this
 461 sense, despite having differences in the viscous corrections, the first order quantities seem
 462 to be quite insensitive to whether one uses the quasiparticle EoS method or the standard
 463 EoS method. That being said, the differences seen in panels (c) and (d) could manifest
 464 themselves as differences in the particle spectra computed along the hypersurface if these
 465 two methods are applied to QGP phenomenology.

466 Finally, in Fig. 6 we present the same four panels, but in the case of an anisotropic initial
 467 condition with an oblate momentum-space anisotropy. As can be seen from Fig. 6, even for
 468 anisotropic initial conditions, the two EoS methods agree extremely well for the evolution
 469 the effective temperature and energy density. However, similar to the case of isotropic initial
 470 conditions, we see somewhat larger differences in the evolution of the pressure anisotropy and

471 qualitative differences in the evolution of the bulk pressure correction. For both quantities,
472 we see that the two methods have the same late-time asymptotic behavior. Finally, we note
473 that the behavior seen in Fig. 6 is indicative of the results we obtained for a variety of
474 different non-equilibrium initial conditions.

475 IX. CONCLUSIONS AND OUTLOOK

476 In this paper, we presented a new method for imposing a realistic EoS in the context
477 of anisotropic hydrodynamics. The method relies on a quasiparticle picture of the QGP,
478 which is conceptually consistent with the kinetic theory method used to derive the re-
479 quired hydrodynamic evolution equations from the Boltzmann equation. We discussed the
480 fact that the introduction of a temperature-dependent quasiparticle mass requires an addi-
481 tional background contribution to the energy-momentum tensor. We showed that requiring
482 energy-momentum conservation results in a constraint equation on the background contribu-
483 tion which reduces to the constraint necessary to enforce thermodynamic consistency in the
484 isotropic equilibrium limit as found by previous authors [10, 11]. When solving the result-
485 ing dynamical equations, we allowed the background contribution to be a non-equilibrium
486 quantity. This was necessary to self-consistently implement the constraint equation.

487 By numerically solving the resulting dynamical equations in the 0+1d, we compared
488 the results obtained using the quasiparticle EoS method with those obtained using the
489 standard method for imposing a realistic EoS in anisotropic hydrodynamics. We found that
490 the temperature evolution obtained using the two methods was nearly identical and that
491 there were only small differences in the pressure anisotropy. However, we found that there
492 were large qualitative differences in the evolution of the bulk pressure correction. These
493 conclusions were supported by the presentation of results for both isotropic and anisotropic
494 initial conditions and also for different values of the shear viscosity to entropy density ratio,
495 however, we internally checked a much larger set of initial conditions/parameter sets and
496 found that these conclusions were generic. We note, however, that the difference in the
497 bulk pressure correction found does not necessarily imply large corrections for heavy-ion
498 phenomenology. As we have shown, first order quantities like the energy density are the
499 same to within a few percent when comparing the two approaches. That being said, the
500 differences in the bulk pressure in particular could be important when fixing the form of the

501 distribution function on the freezeout hypersurface.

502 Looking forward, in a future work we will present numerical comparisons of the two
 503 approaches beyond the simple case of 0+1d expansion considered herein. Additionally, it
 504 would be quite interesting to apply the quasiparticle EoS method to obtain the dynamical
 505 evolution for a non-conformal system with temperature-dependent masses within the context
 506 of second-order viscous hydrodynamics. Finally, we note that it may be possible to construct
 507 exact solutions of the RTA Boltzmann equation for a system of particles with temperature-
 508 dependent masses using methods similar to those in Refs. [74–76]. Additionally, for the case
 509 of quasiparticle masses that are linear in the temperature, it may be possible to exactly
 510 solve the RTA Boltzmann equation subject to Gubser flow similar to Refs. [77, 78].

511 ACKNOWLEDGMENTS

512 We thank W. Florkowski, P. Romatschke, and R. Ryblewski for useful conversations. M.
 513 Strickland and M. Nopoush were supported by the U.S. Department of Energy, Office of
 514 Science, Office of Nuclear Physics under Awards No. DE-SC0013470. M. Alqahtani was
 515 supported by a PhD fellowship from the University of Dammam.

516 Appendix A: Explicit formulas for derivatives

517 In this section, first we introduce the notations used in derivation of the general moment-
 518 based hydrodynamics equations and then, by taking the appropriate limits, we simplify them
 519 for the transversally-homogeneous 0+1d case. Using the definitions

$$\begin{aligned}\mathcal{D} &\equiv \cosh(\vartheta - \varsigma)\partial_\tau + \frac{1}{\tau}\sinh(\vartheta - \varsigma)\partial_\varsigma, \\ \tilde{\mathcal{D}} &\equiv \sinh(\vartheta - \varsigma)\partial_\tau + \frac{1}{\tau}\cosh(\vartheta - \varsigma)\partial_\varsigma,\end{aligned}\tag{A1}$$

$$\nabla_\perp \cdot \mathbf{u}_\perp \equiv \partial_x u_x + \partial_y u_y,$$

$$\mathbf{u}_\perp \cdot \nabla_\perp \equiv u_x \partial_x + u_y \partial_y,$$

$$\mathbf{u}_\perp \times \nabla_\perp \equiv u_x \partial_y - u_y \partial_x,\tag{A2}$$

520 and four-vectors defined in Eq. (8) one has

$$\begin{aligned}
D_u &\equiv u^\mu \partial_\mu = u_0 \mathcal{D} + \mathbf{u}_\perp \cdot \nabla_\perp, \\
D_x &\equiv X^\mu \partial_\mu = u_\perp \mathcal{D} + \frac{u_0}{u_\perp} (\mathbf{u}_\perp \cdot \nabla_\perp), \\
D_y &\equiv Y^\mu \partial_\mu = \frac{1}{u_\perp} (\mathbf{u}_\perp \times \nabla_\perp), \\
D_z &\equiv Z^\mu \partial_\mu = \tilde{\mathcal{D}}.
\end{aligned} \tag{A3}$$

521 The divergences are defined as

$$\begin{aligned}
\theta_u &\equiv \partial_\mu u^\mu = \mathcal{D}u_0 + u_0 \tilde{\mathcal{D}}\vartheta + \nabla_\perp \cdot \mathbf{u}_\perp, \\
\theta_x &\equiv \partial_\mu X^\mu = \mathcal{D}u_\perp + u_\perp \tilde{\mathcal{D}}\vartheta + \frac{u_0}{u_\perp} (\nabla_\perp \cdot \mathbf{u}_\perp) - \frac{1}{u_0 u_\perp^2} (\mathbf{u}_\perp \cdot \nabla_\perp) u_\perp, \\
\theta_y &\equiv \partial_\mu Y^\mu = -\frac{1}{u_\perp} (\mathbf{u}_\perp \cdot \nabla_\perp) \varphi, \\
\theta_z &\equiv \partial_\mu Z^\mu = \mathcal{D}\vartheta,
\end{aligned} \tag{A4}$$

522 where $\varphi = \tan^{-1}(u_y/u_x)$.

$$\begin{aligned}
u_\mu D_\alpha X^\mu &= \frac{1}{u_0} D_\alpha u_\perp, \\
u_\mu D_\alpha Y^\mu &= u_\perp D_\alpha \varphi, \\
u_\mu D_\alpha Z^\mu &= u_0 D_\alpha \vartheta, \\
X_\mu D_\alpha Y^\mu &= u_0 D_\alpha \varphi, \\
X_\mu D_\alpha Z^\mu &= u_\perp D_\alpha \vartheta, \\
Y_\mu D_\alpha Z^\mu &= 0,
\end{aligned} \tag{A5}$$

523 where $\alpha \in \{u, x, y, z\}$. Note that contractions such as $X^\mu D_\alpha u_\mu$ are also non-vanishing, how-
524 ever, such terms can be written in terms of the expressions above by using the orthogonality
525 of the basis vectors, i.e. $D_\alpha(X^\mu u_\mu) = 0$ implies that $X^\mu D_\alpha u_\mu = -u_\mu D_\alpha X^\mu$.

1. Simplification for 1+1d

In the case of boost-invariant and cylindrically-symmetric flow one has $\varphi \rightarrow \phi$ and $\vartheta \rightarrow \varsigma$,

where ς is the spatial rapidity. Using $u_\perp \equiv \sinh \theta_\perp$, one can rewrite (A2) as

$$\begin{aligned}
\mathcal{D} &= \partial_\tau, \\
\tilde{\mathcal{D}} &= \frac{1}{\tau} \partial_\varsigma, \\
\nabla_\perp \cdot \mathbf{u}_\perp &= \partial_r u_\perp + \frac{u_\perp}{r}, \\
\mathbf{u}_\perp \cdot \nabla_\perp &= u_\perp \partial_r, \\
\mathbf{u}_\perp \times \nabla_\perp &= \frac{u_\perp}{r} \partial_\phi.
\end{aligned} \tag{A6}$$

Also, the identities in (A4) become

$$D_u = \cosh \theta_\perp \partial_\tau + \sinh \theta_\perp \partial_r, \tag{A7}$$

$$D_x = \sinh \theta_\perp \partial_\tau + \cosh \theta_\perp \partial_r, \tag{A8}$$

$$D_y = \frac{1}{r} \partial_\phi, \tag{A9}$$

$$D_z = \frac{1}{\tau} \partial_\varsigma, \tag{A10}$$

$$\theta_u = \cosh \theta_\perp \left(\frac{1}{\tau} + \partial_r \theta_\perp \right) + \sinh \theta_\perp \left(\frac{1}{r} + \partial_\tau \theta_\perp \right), \tag{A11}$$

$$\theta_x = \sinh \theta_\perp \left(\frac{1}{\tau} + \partial_r \theta_\perp \right) + \cosh \theta_\perp \left(\frac{1}{r} + \partial_\tau \theta_\perp \right), \tag{A12}$$

$$\theta_y = \theta_z = 0. \tag{A13}$$

In this limit, the only non-vanishing terms in (A5) are

$$\begin{aligned}
u_\mu D_u X^\mu &= D_u \theta_\perp, \\
u_\mu D_x X^\mu &= D_x \theta_\perp, \\
u_\mu D_y Y^\mu &= \frac{1}{r} \sinh \theta_\perp, \\
u_\mu D_z Z^\mu &= \frac{1}{\tau} \cosh \theta_\perp, \\
X_\mu D_y Y^\mu &= \frac{1}{r} \cosh \theta_\perp, \\
X_\mu D_z Z^\mu &= \frac{1}{\tau} \sinh \theta_\perp.
\end{aligned} \tag{A14}$$

531

2. Simplification for 0+1d

532

For this case, one has $\theta_\perp = 0$ and

$$D_u = \partial_\tau, \quad (\text{A15})$$

$$D_x = \partial_r, \quad (\text{A16})$$

$$D_y = \frac{\partial_\phi}{r}, \quad (\text{A17})$$

$$D_z = \frac{\partial_\zeta}{\tau}, \quad (\text{A18})$$

$$\theta_u = \frac{1}{\tau}, \quad (\text{A19})$$

$$\theta_x = \frac{1}{r}, \quad (\text{A20})$$

$$\theta_y = \theta_z = 0. \quad (\text{A21})$$

533

In this limit, the only non-vanishing terms in (A5) are

$$u_\mu D_z Z^\mu = \frac{1}{\tau},$$

$$X_\mu D_y Y^\mu = \frac{1}{r}.$$

534

Appendix B: special functions

535

In this section, we provide definitions of the special functions appearing in the body of

536

the text. We start by introducing

$$\begin{aligned} \mathcal{H}_2(y, z) &\equiv y \int_{-1}^1 dx \sqrt{(y^2 - 1)x^2 + z^2 + 1} \\ &= \frac{y}{\sqrt{y^2 - 1}} \left[(z^2 + 1) \tanh^{-1} \sqrt{\frac{y^2 - 1}{y^2 + z^2}} + \sqrt{(y^2 - 1)(y^2 + z^2)} \right], \end{aligned} \quad (\text{B1})$$

537

$$\begin{aligned} \mathcal{H}_{2T}(y, z) &\equiv y \int_{-1}^1 \frac{dx(1 - x^2)}{\sqrt{(y^2 - 1)x^2 + z^2 + 1}} \\ &= \frac{y}{(y^2 - 1)^{3/2}} \left[(z^2 + 2y^2 - 1) \tanh^{-1} \sqrt{\frac{y^2 - 1}{y^2 + z^2}} - \sqrt{(y^2 - 1)(y^2 + z^2)} \right], \end{aligned} \quad (\text{B2})$$

$$\begin{aligned}\mathcal{H}_{2L}(y, z) &\equiv y^3 \int_{-1}^1 \frac{dx x^2}{\sqrt{(y^2 - 1)x^2 + z^2 + 1}} \\ &= \frac{y^3}{(y^2 - 1)^{3/2}} \left[\sqrt{(y^2 - 1)(y^2 + z^2)} - (z^2 + 1) \tanh^{-1} \sqrt{\frac{y^2 - 1}{y^2 + z^2}} \right].\end{aligned}\quad (\text{B3})$$

539 Derivatives of these functions satisfy the following relations

$$\frac{\partial \mathcal{H}_2(y, z)}{\partial y} = \frac{1}{y} \left[\mathcal{H}_2(y, z) + \mathcal{H}_{2L}(y, z) \right], \quad (\text{B4})$$

$$\frac{\partial \mathcal{H}_2(y, z)}{\partial z} = \frac{1}{z} \left[\mathcal{H}_2(y, z) - \mathcal{H}_{2L}(y, z) - \mathcal{H}_{2T}(y, z) \right]. \quad (\text{B5})$$

540 1. Massive Case

541 The \mathcal{H} -functions appearing in the definitions of components of the energy-momentum
542 tensor are

$$\mathcal{H}_3(\boldsymbol{\alpha}, \hat{m}) \equiv \tilde{N} \alpha_x \alpha_y \int_0^{2\pi} d\phi \alpha_\perp^2 \int_0^\infty d\hat{p} \hat{p}^3 f_{\text{eq}}(\sqrt{\hat{p}^2 + \hat{m}^2}) \mathcal{H}_2\left(\frac{\alpha_z}{\alpha_\perp}, \frac{\hat{m}}{\alpha_\perp \hat{p}}\right), \quad (\text{B6})$$

$$\mathcal{H}_{3x}(\boldsymbol{\alpha}, \hat{m}) \equiv \tilde{N} \alpha_x^3 \alpha_y \int_0^{2\pi} d\phi \cos^2 \phi \int_0^\infty d\hat{p} \hat{p}^3 f_{\text{eq}}(\sqrt{\hat{p}^2 + \hat{m}^2}) \mathcal{H}_{2T}\left(\frac{\alpha_z}{\alpha_\perp}, \frac{\hat{m}}{\alpha_\perp \hat{p}}\right), \quad (\text{B7})$$

$$\mathcal{H}_{3y}(\boldsymbol{\alpha}, \hat{m}) \equiv \tilde{N} \alpha_x \alpha_y^3 \int_0^{2\pi} d\phi \sin^2 \phi \int_0^\infty d\hat{p} \hat{p}^3 f_{\text{eq}}(\sqrt{\hat{p}^2 + \hat{m}^2}) \mathcal{H}_{2T}\left(\frac{\alpha_z}{\alpha_\perp}, \frac{\hat{m}}{\alpha_\perp \hat{p}}\right), \quad (\text{B8})$$

$$\mathcal{H}_{3T}(\boldsymbol{\alpha}, \hat{m}) \equiv \frac{1}{2} \left[\mathcal{H}_{3x}(\boldsymbol{\alpha}, \hat{m}) + \mathcal{H}_{3y}(\boldsymbol{\alpha}, \hat{m}) \right], \quad (\text{B9})$$

$$\mathcal{H}_{3L}(\boldsymbol{\alpha}, \hat{m}) \equiv \tilde{N} \alpha_x \alpha_y \int_0^{2\pi} d\phi \alpha_\perp^2 \int_0^\infty d\hat{p} \hat{p}^3 f_{\text{eq}}(\sqrt{\hat{p}^2 + \hat{m}^2}) \mathcal{H}_{2L}\left(\frac{\alpha_z}{\alpha_\perp}, \frac{\hat{m}}{\alpha_\perp \hat{p}}\right), \quad (\text{B10})$$

$$\mathcal{H}_{3m}(\boldsymbol{\alpha}, \hat{m}) \equiv \tilde{N} \alpha_x \alpha_y \hat{m}^2 \int_0^{2\pi} d\phi \alpha_\perp^2 \int_0^\infty d\hat{p} \hat{p}^3 \frac{f_{\text{eq}}(\sqrt{\hat{p}^2 + \hat{m}^2})}{\sqrt{\hat{p}^2 + \hat{m}^2}} \mathcal{H}_2\left(\frac{\alpha_z}{\alpha_\perp}, \frac{\hat{m}}{\alpha_\perp \hat{p}}\right), \quad (\text{B11})$$

$$\mathcal{H}_{3B}(\boldsymbol{\alpha}, \hat{m}) \equiv \tilde{N} \alpha_x \alpha_y \int_0^{2\pi} d\phi \int_0^\infty d\hat{p} \hat{p} f_{\text{eq}}(\sqrt{\hat{p}^2 + \hat{m}^2}) \mathcal{H}_{2B}\left(\frac{\alpha_z}{\alpha_\perp}, \frac{\hat{m}}{\alpha_\perp \hat{p}}\right), \quad (\text{B12})$$

$$\Omega_T(\boldsymbol{\alpha}, \hat{m}) \equiv \mathcal{H}_3 + \mathcal{H}_{3T}, \quad (\text{B13})$$

$$\Omega_L(\boldsymbol{\alpha}, \hat{m}) \equiv \mathcal{H}_3 + \mathcal{H}_{3L}, \quad (\text{B14})$$

$$\Omega_m(\boldsymbol{\alpha}, \hat{m}) \equiv \mathcal{H}_3 - \mathcal{H}_{3L} - 2\mathcal{H}_{3T} - \mathcal{H}_{3m}, \quad (\text{B15})$$

543 where $\alpha_{\perp}^2 \equiv \alpha_x^2 \cos^2 \phi + \alpha_y^2 \sin^2 \phi$ and

$$\mathcal{H}_{2B}(y, z) \equiv \mathcal{H}_{2T}(y, z) + \frac{\mathcal{H}_{2L}(y, z)}{y^2} = \frac{2}{\sqrt{y^2 - 1}} \tanh^{-1} \sqrt{\frac{y^2 - 1}{y^2 + z^2}}. \quad (\text{B16})$$

544 Also, derivatives of \mathcal{H}_3 satisfy

$$\frac{\partial \mathcal{H}_3}{\partial \alpha_x} = \frac{2}{\alpha_x} \Omega_T, \quad (\text{B17})$$

$$\frac{\partial \mathcal{H}_3}{\partial \alpha_z} = \frac{1}{\alpha_z} \Omega_L, \quad (\text{B18})$$

$$\frac{\partial \mathcal{H}_3}{\partial \hat{m}} = \frac{1}{\hat{m}} \Omega_m. \quad (\text{B19})$$

545 For a 0+1d system one has $\alpha_x = \alpha_y$ such that $\alpha_{\perp} = \alpha_x$ and $\tilde{\mathcal{H}}_{3T} \equiv \tilde{\mathcal{H}}_{3x} = \tilde{\mathcal{H}}_{3y}$, so that one
546 obtains

$$\tilde{\mathcal{H}}_3(\boldsymbol{\alpha}, \hat{m}) \equiv 2\pi \tilde{N} \alpha_x^4 \int_0^{\infty} d\hat{p} \hat{p}^3 f_{\text{eq}}(\sqrt{\hat{p}^2 + \hat{m}^2}) \mathcal{H}_2\left(\frac{\alpha_z}{\alpha_x}, \frac{\hat{m}}{\alpha_x \hat{p}}\right), \quad (\text{B20})$$

$$\tilde{\mathcal{H}}_{3T}(\boldsymbol{\alpha}, \hat{m}) \equiv \pi \tilde{N} \alpha_x^4 \int_0^{\infty} d\hat{p} \hat{p}^3 f_{\text{eq}}(\sqrt{\hat{p}^2 + \hat{m}^2}) \mathcal{H}_{2T}\left(\frac{\alpha_z}{\alpha_x}, \frac{\hat{m}}{\alpha_x \hat{p}}\right), \quad (\text{B21})$$

$$\tilde{\mathcal{H}}_{3L}(\boldsymbol{\alpha}, \hat{m}) \equiv 2\pi \tilde{N} \alpha_x^4 \int_0^{\infty} d\hat{p} \hat{p}^3 f_{\text{eq}}(\sqrt{\hat{p}^2 + \hat{m}^2}) \mathcal{H}_{2L}\left(\frac{\alpha_z}{\alpha_x}, \frac{\hat{m}}{\alpha_x \hat{p}}\right), \quad (\text{B22})$$

$$\tilde{\mathcal{H}}_{3m}(\boldsymbol{\alpha}, \hat{m}) \equiv 2\pi \tilde{N} \alpha_x^4 \hat{m}^2 \int_0^{\infty} d\hat{p} \hat{p}^3 \frac{f_{\text{eq}}(\sqrt{\hat{p}^2 + \hat{m}^2})}{\sqrt{\hat{p}^2 + \hat{m}^2}} \mathcal{H}_2\left(\frac{\alpha_z}{\alpha_x}, \frac{\hat{m}}{\alpha_x \hat{p}}\right), \quad (\text{B23})$$

$$\mathcal{H}_{3B}(\boldsymbol{\alpha}, \hat{m}) \equiv 2\pi \tilde{N} \alpha_x^2 \int_0^{\infty} d\hat{p} \hat{p} f_{\text{eq}}(\sqrt{\hat{p}^2 + \hat{m}^2}) \mathcal{H}_{2B}\left(\frac{\alpha_z}{\alpha_x}, \frac{\hat{m}}{\alpha_x \hat{p}}\right). \quad (\text{B24})$$

547 For the isotropic equilibrium case, one has $\alpha_i \rightarrow 1$, $\lambda \rightarrow T$, and $\hat{m} \rightarrow \hat{m}_{\text{eq}}$

$$\tilde{\mathcal{H}}_{3,\text{eq}}(\hat{m}_{\text{eq}}) = 4\pi \tilde{N} \hat{m}_{\text{eq}}^2 \left[\hat{m}_{\text{eq}} K_1(\hat{m}_{\text{eq}}) + 3K_2(\hat{m}_{\text{eq}}) \right], \quad (\text{B25})$$

$$\tilde{\mathcal{H}}_{3T,\text{eq}}(\hat{m}_{\text{eq}}) = \tilde{\mathcal{H}}_{3L,\text{eq}}(\hat{m}_{\text{eq}}) = 4\pi \tilde{N} \hat{m}_{\text{eq}}^2 K_2(\hat{m}_{\text{eq}}), \quad (\text{B26})$$

$$\tilde{\mathcal{H}}_{3m,\text{eq}}(\hat{m}_{\text{eq}}) = 4\pi \tilde{N} \hat{m}_{\text{eq}}^4 K_2(\hat{m}_{\text{eq}}). \quad (\text{B27})$$

2. Massless Case

Taking the massless limit of Eqs. (B6) - (B12) one obtains

$$\hat{\mathcal{H}}_3(\boldsymbol{\alpha}) \equiv \lim_{m \rightarrow 0} \mathcal{H}_3(\boldsymbol{\alpha}, \hat{m}) = 6\tilde{N}\alpha_x\alpha_y \int_0^{2\pi} d\phi \alpha_\perp^2 \bar{\mathcal{H}}_2\left(\frac{\alpha_z}{\alpha_\perp}\right), \quad (\text{B28})$$

$$\hat{\mathcal{H}}_{3x}(\boldsymbol{\alpha}) \equiv \lim_{m \rightarrow 0} \mathcal{H}_{3x}(\boldsymbol{\alpha}, \hat{m}) = 6\tilde{N}\alpha_x^3\alpha_y \int_0^{2\pi} d\phi \cos^2 \phi \bar{\mathcal{H}}_{2T}\left(\frac{\alpha_z}{\alpha_\perp}\right), \quad (\text{B29})$$

$$\hat{\mathcal{H}}_{3y}(\boldsymbol{\alpha}) \equiv \lim_{m \rightarrow 0} \mathcal{H}_{3y}(\boldsymbol{\alpha}, \hat{m}) = 6\tilde{N}\alpha_x\alpha_y^3 \int_0^{2\pi} d\phi \sin^2 \phi \bar{\mathcal{H}}_{2T}\left(\frac{\alpha_z}{\alpha_\perp}\right), \quad (\text{B30})$$

$$\hat{\mathcal{H}}_{3L}(\boldsymbol{\alpha}) \equiv \lim_{m \rightarrow 0} \mathcal{H}_{3L}(\boldsymbol{\alpha}, \hat{m}) = 6\tilde{N}\alpha_x\alpha_y \int_0^{2\pi} d\phi \alpha_\perp^2 \bar{\mathcal{H}}_{2L}\left(\frac{\alpha_z}{\alpha_\perp}\right), \quad (\text{B31})$$

$$\hat{\mathcal{H}}_{3m}(\boldsymbol{\alpha}) \equiv \lim_{m \rightarrow 0} \mathcal{H}_{3m}(\boldsymbol{\alpha}, \hat{m}) = 0, \quad (\text{B32})$$

550 where $\bar{\mathcal{H}}_{2,2T,2L}(y) \equiv \mathcal{H}_{2,2T,2L}(y, 0)$. In the transversally-symmetric case, $\alpha_x = \alpha_y$ and $\bar{\mathcal{H}}_{3T} \equiv$

551 $\bar{\mathcal{H}}_{3x} = \bar{\mathcal{H}}_{3y}$, and the functions above simplify to

$$\bar{\mathcal{H}}_3(\boldsymbol{\alpha}) = 12\pi\tilde{N}\alpha_x^4\bar{\mathcal{H}}_2\left(\frac{\alpha_z}{\alpha_x}\right), \quad (\text{B33})$$

$$\bar{\mathcal{H}}_{3T}(\boldsymbol{\alpha}) = 6\pi\tilde{N}\alpha_x^4\bar{\mathcal{H}}_{2T}\left(\frac{\alpha_z}{\alpha_x}\right), \quad (\text{B34})$$

$$\bar{\mathcal{H}}_{3L}(\boldsymbol{\alpha}) = 12\pi\tilde{N}\alpha_x^4\bar{\mathcal{H}}_{2L}\left(\frac{\alpha_z}{\alpha_x}\right). \quad (\text{B35})$$

552 In the isotropic equilibrium case, one has $\alpha_i \rightarrow 1$ and $\lambda \rightarrow T$, and, as a result,

$$\bar{\mathcal{H}}_{3,\text{eq}} = 24\pi\tilde{N}, \quad (\text{B36})$$

$$\bar{\mathcal{H}}_{3T,\text{eq}} = \bar{\mathcal{H}}_{3L,\text{eq}}(\boldsymbol{\alpha}) = 8\pi\tilde{N}. \quad (\text{B37})$$

[1] E. Braaten and R. D. Pisarski, *Nucl. Phys.* **B337**, 569 (1990).

[2] J. O. Andersen, E. Braaten, and M. Strickland, *Phys. Rev. Lett.* **83**, 2139 (1999), arXiv:hep-ph/9902327 [hep-ph].

[3] J. O. Andersen, E. Petitgirard, and M. Strickland, *Phys.Rev.* **D70**, 045001 (2004), arXiv:hep-ph/0302069 [hep-ph].

[4] J. O. Andersen and M. Strickland, *Annals Phys.* **317**, 281 (2005), arXiv:hep-ph/0404164 [hep-ph].

- 560 [5] J. O. Andersen, L. E. Leganger, M. Strickland, and N. Su, *JHEP* **08**, 053 (2011),
561 [arXiv:1103.2528 \[hep-ph\]](#).
- 562 [6] N. Haque, A. Bandyopadhyay, J. O. Andersen, M. G. Mustafa, M. Strickland, and N. Su,
563 *JHEP* **05**, 027 (2014), [arXiv:1402.6907 \[hep-ph\]](#).
- 564 [7] R. Bellwied, S. Borsanyi, Z. Fodor, S. D. Katz, A. Pasztor, C. Ratti, and K. K. Szabo, (2015),
565 [arXiv:1507.04627 \[hep-lat\]](#).
- 566 [8] H. T. Ding, S. Mukherjee, H. Ohno, P. Petreczky, and H. P. Schadler, (2015),
567 [arXiv:1507.06637 \[hep-lat\]](#).
- 568 [9] M. I. Gorenstein and S. N. Yang, *Physical Review D* **52**, 5206 (1995).
- 569 [10] S. Jeon and L. G. Yaffe, *Phys.Rev.* **D53**, 5799 (1996), [arXiv:hep-ph/9512263 \[hep-ph\]](#).
- 570 [11] P. Romatschke, *Phys.Rev.* **D85**, 065012 (2012), [arXiv:1108.5561 \[gr-qc\]](#).
- 571 [12] P. Huovinen, P. F. Kolb, U. W. Heinz, P. V. Ruuskanen, and S. A. Voloshin, *Phys. Lett.*
572 **B503**, 58 (2001), [arXiv:hep-ph/0101136](#).
- 573 [13] T. Hirano and K. Tsuda, *Phys. Rev.* **C66**, 054905 (2002), [arXiv:nucl-th/0205043](#).
- 574 [14] P. F. Kolb and U. W. Heinz, In Hwa, R.C. (ed.) et al.: *Quark gluon plasma* , 634 (2003),
575 [arXiv:nucl-th/0305084](#).
- 576 [15] A. Muronga, *Phys. Rev. Lett.* **88**, 062302 (2002), [arXiv:nucl-th/0104064](#).
- 577 [16] A. Muronga, *Phys. Rev.* **C69**, 034903 (2004), [arXiv:nucl-th/0309055](#).
- 578 [17] A. Muronga and D. H. Rischke, (2004), [arXiv:nucl-th/0407114 \[nucl-th\]](#).
- 579 [18] U. W. Heinz, H. Song, and A. K. Chaudhuri, *Phys.Rev.* **C73**, 034904 (2006), [arXiv:nucl-](#)
580 [th/0510014 \[nucl-th\]](#).
- 581 [19] R. Baier, P. Romatschke, and U. A. Wiedemann, *Phys.Rev.* **C73**, 064903 (2006), [arXiv:hep-](#)
582 [ph/0602249 \[hep-ph\]](#).
- 583 [20] P. Romatschke and U. Romatschke, *Phys. Rev. Lett.* **99**, 172301 (2007), [arXiv:0706.1522](#)
584 [\[nucl-th\]](#).
- 585 [21] R. Baier, P. Romatschke, D. T. Son, A. O. Starinets, and M. A. Stephanov, *JHEP* **0804**, 100
586 (2008), [arXiv:0712.2451 \[hep-th\]](#).
- 587 [22] K. Dusling and D. Teaney, *Phys. Rev.* **C77**, 034905 (2008), [arXiv:0710.5932 \[nucl-th\]](#).
- 588 [23] M. Luzum and P. Romatschke, *Phys. Rev.* **C78**, 034915 (2008), [arXiv:0804.4015 \[nucl-th\]](#).
- 589 [24] H. Song and U. W. Heinz, *J.Phys.G* **G36**, 064033 (2009), [arXiv:0812.4274 \[nucl-th\]](#).

- 590 [25] U. W. Heinz, Relativistic Heavy Ion Physics, Landolt-Boernstein New Series, I/23, edited by
591 R. Stock, Springer Verlag, New York, Chap. 5 (2010), [arXiv:0901.4355 \[nucl-th\]](#).
- 592 [26] P. Bozek and I. Wyskiel, *Phys.Rev.* **C79**, 044916 (2009), [arXiv:0902.4121 \[nucl-th\]](#).
- 593 [27] P. Bozek, *Phys.Rev.* **C81**, 034909 (2010), [arXiv:0911.2397 \[nucl-th\]](#).
- 594 [28] A. El, Z. Xu, and C. Greiner, *Phys. Rev.* **C81**, 041901 (2010), [arXiv:0907.4500 \[hep-ph\]](#).
- 595 [29] J. Peralta-Ramos and E. Calzetta, *Phys. Rev.* **D80**, 126002 (2009), [arXiv:0908.2646 \[hep-ph\]](#).
- 596 [30] J. Peralta-Ramos and E. Calzetta, *Phys.Rev.* **C82**, 054905 (2010), [arXiv:1003.1091 \[hep-ph\]](#).
- 597 [31] G. Denicol, T. Kodama, and T. Koide, *J.Phys.G* **G37**, 094040 (2010), [arXiv:1002.2394 \[nucl-](#)
598 [th\]](#).
- 599 [32] G. Denicol, T. Koide, and D. Rischke, *Phys.Rev.Lett.* **105**, 162501 (2010), [arXiv:1004.5013](#)
600 [\[nucl-th\]](#).
- 601 [33] B. Schenke, S. Jeon, and C. Gale, *Phys.Rev.Lett.* **106**, 042301 (2011), [arXiv:1009.3244 \[hep-](#)
602 [ph\]](#).
- 603 [34] B. Schenke, S. Jeon, and C. Gale, *Phys.Lett.* **B702**, 59 (2011), [arXiv:1102.0575 \[hep-ph\]](#).
- 604 [35] P. Bozek, *Phys.Lett.* **B699**, 283 (2011), [arXiv:1101.1791 \[nucl-th\]](#).
- 605 [36] P. Bozek, *Phys.Rev.* **C85**, 034901 (2012), [arXiv:1110.6742 \[nucl-th\]](#).
- 606 [37] H. Niemi, G. S. Denicol, P. Huovinen, E. Molnár, and D. H. Rischke, *Phys.Rev.Lett.* **106**,
607 [212302 \(2011\)](#), [arXiv:1101.2442 \[nucl-th\]](#).
- 608 [38] H. Niemi, G. S. Denicol, P. Huovinen, E. Molnár, and D. H. Rischke, *Phys. Rev. C* **86**, 014909
609 [\(2012\)](#).
- 610 [39] P. Bożek and I. Wyskiel-Piekarska, *Phys. Rev. C* **85**, 064915 (2012).
- 611 [40] G. S. Denicol, H. Niemi, E. Molnár, and D. H. Rischke, *Phys. Rev. D* **85**, 114047 (2012).
- 612 [41] G. Denicol, E. Molnár, H. Niemi, and D. Rischke, *Eur. Phys. J. A* **48**, 170 (2012),
613 [arXiv:1206.1554 \[nucl-th\]](#).
- 614 [42] J. Peralta-Ramos and E. Calzetta, *Phys.Rev.* **D87**, 034003 (2013), [arXiv:1212.0824 \[nucl-th\]](#).
- 615 [43] E. Calzetta, *Phys. Rev.* **D92**, 045035 (2015), [arXiv:1402.5278 \[hep-ph\]](#).
- 616 [44] G. S. Denicol, S. Jeon, and C. Gale, *Phys. Rev.* **C90**, 024912 (2014), [arXiv:1403.0962 \[nucl-th\]](#).
- 617 [45] W. Florkowski, A. Jaiswal, E. Maksymiuk, R. Ryblewski, and M. Strickland, *Phys. Rev.*
618 [C91](#), 054907 (2015), [arXiv:1503.03226 \[nucl-th\]](#).
- 619 [46] S. Ryu, J. F. Paquet, C. Shen, G. Denicol, B. Schenke, *et al.*, (2015), [arXiv:1502.01675](#)
620 [\[nucl-th\]](#).

- 621 [47] M. Martinez and M. Strickland, *Nucl. Phys.* **A848**, 183 (2010), arXiv:1007.0889 [nucl-th].
- 622 [48] W. Florkowski and R. Ryblewski, *Phys.Rev.* **C83**, 034907 (2011), arXiv:1007.0130 [nucl-th].
- 623 [49] R. Ryblewski and W. Florkowski, *J.Phys.G* **G38**, 015104 (2011), arXiv:1007.4662 [nucl-th].
- 624 [50] M. Martinez and M. Strickland, *Nucl.Phys.* **A856**, 68 (2011), arXiv:1011.3056 [nucl-th].
- 625 [51] R. Ryblewski and W. Florkowski, *Eur.Phys.J.* **C71**, 1761 (2011), arXiv:1103.1260 [nucl-th].
- 626 [52] W. Florkowski and R. Ryblewski, *Phys.Rev.* **C85**, 044902 (2012), arXiv:1111.5997 [nucl-th].
- 627 [53] M. Martinez, R. Ryblewski, and M. Strickland, *Phys.Rev.* **C85**, 064913 (2012),
628 arXiv:1204.1473 [nucl-th].
- 629 [54] R. Ryblewski and W. Florkowski, *Phys. Rev.* **C85**, 064901 (2012), arXiv:1204.2624 [nucl-th].
- 630 [55] W. Florkowski, R. Maj, R. Ryblewski, and M. Strickland, *Phys.Rev.* **C87**, 034914 (2013),
631 arXiv:1209.3671 [nucl-th].
- 632 [56] W. Florkowski and R. Maj, *Acta Phys.Polon.* **B44**, 2003 (2013), arXiv:1309.2786 [nucl-th].
- 633 [57] R. Ryblewski, *J.Phys.* **G40**, 093101 (2013).
- 634 [58] D. Bazow, U. W. Heinz, and M. Strickland, *Phys.Rev.* **C90**, 054910 (2014), arXiv:1311.6720
635 [nucl-th].
- 636 [59] L. Tinti and W. Florkowski, *Phys.Rev.* **C89**, 034907 (2014), arXiv:1312.6614 [nucl-th].
- 637 [60] W. Florkowski, R. Ryblewski, M. Strickland, and L. Tinti, *Phys.Rev.* **C89**, 054909 (2014),
638 arXiv:1403.1223 [hep-ph].
- 639 [61] W. Florkowski and O. Madetko, *Acta Phys.Polon.* **B45**, 1103 (2014), arXiv:1402.2401 [nucl-
640 th].
- 641 [62] M. Nopoush, R. Ryblewski, and M. Strickland, *Phys.Rev.* **C90**, 014908 (2014),
642 arXiv:1405.1355 [hep-ph].
- 643 [63] G. S. Denicol, W. Florkowski, R. Ryblewski, and M. Strickland, *Phys.Rev.* **C90**, 044905
644 (2014), arXiv:1407.4767 [hep-ph].
- 645 [64] L. Tinti, R. Ryblewski, W. Florkowski, and M. Strickland, (2015), arXiv:1505.06456 [hep-ph].
- 646 [65] D. Bazow, U. W. Heinz, and M. Martinez, *Phys.Rev.* **C91**, 064903 (2015), arXiv:1503.07443
647 [nucl-th].
- 648 [66] M. Nopoush, M. Strickland, R. Ryblewski, D. Bazow, U. Heinz, and M. Martinez, (2015),
649 arXiv:1506.05278 [nucl-th].
- 650 [67] D. Bazow, M. Martinez, and U. W. Heinz, (2015), arXiv:1507.06595 [nucl-th].

- 651 [68] W. Florkowski, E. Maksymiuk, R. Ryblewski, and L. Tinti, (2015), [arXiv:1508.04534](#) [nucl-
652 th].
- 653 [69] M. Strickland, *Acta Phys. Polon.* **B45**, 2355 (2014), [arXiv:1410.5786](#) [nucl-th].
- 654 [70] S. Borsanyi, G. Endrodi, Z. Fodor, A. Jakovac, S. D. Katz, *et al.*, *JHEP* **1011**, 077 (2010),
655 [arXiv:1007.2580](#) [hep-lat].
- 656 [71] J. Anderson and H. Witting, *Physica* **74**, 489 (1974).
- 657 [72] W. Czyz and W. Florkowski, *Acta Phys. Polon.* **B17**, 819 (1986).
- 658 [73] J. Berges and S. Borsanyi, *Phys. Rev.* **D74**, 045022 (2006), [arXiv:hep-ph/0512155](#) [hep-ph].
- 659 [74] W. Florkowski, R. Ryblewski, and M. Strickland, *Nucl. Phys.* **A916**, 249 (2013),
660 [arXiv:1304.0665](#) [nucl-th].
- 661 [75] W. Florkowski, R. Ryblewski, and M. Strickland, *Phys. Rev.* **C88**, 024903 (2013),
662 [arXiv:1305.7234](#) [nucl-th].
- 663 [76] W. Florkowski, E. Maksymiuk, R. Ryblewski, and M. Strickland, *Phys. Rev.* **C89**, 054908
664 (2014), [arXiv:1402.7348](#) [hep-ph].
- 665 [77] G. S. Denicol, U. W. Heinz, M. Martinez, J. Noronha, and M. Strickland, *Phys. Rev. Lett.*
666 **113**, 202301 (2014), [arXiv:1408.5646](#) [hep-ph].
- 667 [78] G. S. Denicol, U. W. Heinz, M. Martinez, J. Noronha, and M. Strickland, *Phys. Rev.* **D90**,
668 125026 (2014), [arXiv:1408.7048](#) [hep-ph].